5-2022

Studying Acetylation of Aconitase Isozymes by Genetic Code Expansion

Jessica Araujo
University of Arkansas, Fayetteville

Studying Acetylation of Aconitase Isozymes by Genetic Code Expansion

A thesis submitted in partial fulfillment
of the requirements for the degree of
Master of Science in Cell and Molecular Biology

by

Jessica Araujo
University of Arkansas Fort Smith
Bachelor of Science in Chemistry, 2019

May 2022
University of Arkansas

This thesis is approved for recommendation to the Graduate Council.

_____
Chenguang Fan, Ph.D.
Dissertation Director

_____
Josh Sakon, Ph.D.
Committee Member

_____
Yuchun Du, Ph.D.
Committee Member

Abstract

The tricarboxylic acid (TCA) cycle is a very important, centrally located, energy-producing pathway that connects numerous other metabolic and regulatory pathways. Enzymes of this cycle have been more recently implicated in various cancers and neurometabolic disorders, however, the exact mechanism by which this happens becomes quite complex when considering the potential modification of these enzymes and the presence of multiple forms of the enzymes and therefore there is much to be studied in this area.

Aconitase has become a recent enzyme of interest as its substrate, citrate, has been found to play a major role in many vital processes within an organism, including the survival and expansion of cancer. Additionally, the modification of aconitase by acetylation has been recently found to drive its activation to support energy, growth, and metastasis in prostate cancer tissue.

In this master's thesis, I apply the genetic code expansion technique to *E. coli* aconitase isozymes AcnA and AcnB to examine the changes in function caused by the modification of the structure in order to achieve a greater understanding of the impact of lysine acetylation in these isozymes.

Acknowledgments

I would like to first thank my advisor Dr. Chenguang Fan for encouraging me as a new researcher. His guidance as a mentor throughout this program has been invaluable. Thank you, Dr. Fan, for welcoming me into your lab.

Thank you to Professor Du and Professor Sakon, for devoting their time to serve on my committee.

A big thank you to my friends and family, who have helped keep my spirits high.

Finally, I would like to give special thanks to my husband Henry for supporting me during this program. His love and support were never wavering through the highs and lows of these past couple of years of my education.

Table of Contents

List of Published Papers

Chapter 2

Jessica Araujo, Sara Ottinger, Sumana Venkat, Qinglei Gan, Chenguang Fan*. Studying acetylation of aconitase isozymes by genetic code expansion. Front. Chem. 2022; 10:862483.) Published

CHAPTER I

Introduction

1.1 Tricarboxylic Acid Cycle

Mitochondria are folded and complex organelles surrounded by a simple outer membrane. The space inside the inner membrane is known as the matrix, and the space between the inner and outer membranes is referred to as the intermembrane space. Most of the enzymes of energy production are found in the matrix, while many enzymes that utilize ATP are found in the intermembrane space. About 150 different mitochondrial diseases involving enzyme dysfunction have been reported. With such a vital role in energy production and consumption, defects arising from mitochondrial enzyme dysfunction are quite serious and affected human embryos rarely survive to see birth.

The tricarboxylic acid (TCA) cycle or the citric acid cycle, more commonly called the Kreb's cycle, is a series of eight enzymes that are found in the mitochondrial matrix—with the exception of succinate dehydrogenase, which is found in the inner membrane, to produce adenosine triphosphate (ATP) and carbon dioxide (CO_2) from the oxidation of acetyl-CoA derived from fats, carbohydrates and lipids. Molecules of NADH and $FADH_2$ are produced throughout the course of this cycle to be used by eukaryotes to create more energy via the electron transport chain in the inner mitochondrial membrane.[1] The TCA cycle supplies energy via oxidative catabolism and also produces intermediates for other biosynthetic processes such as gluconeogenesis, transamination, deamination and fatty acid synthesis.[2] This makes the TCA cycle a very important centrally- located pathway that connects numerous other metabolic pathways (**Figure 1.1**). There is an emerging role of the TCA- cycle related enzymes in human

diseases such as neurometabolic disorders and tumors, however the role of these enzymes is not fully understood.[3]

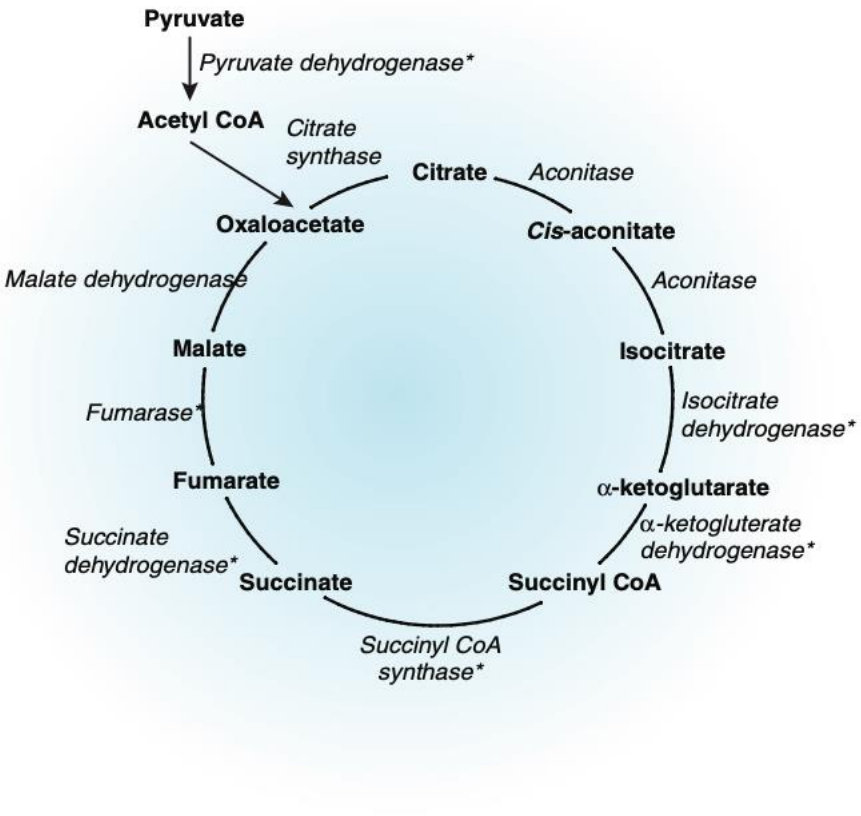

Figure 1.1. The TCA cycle shown with enzymes in italics. Asterisks indicate known enzymopathies as of 2008 reviewed by Munnich "Casting an eye on the Krebs cycle.[4]"

1.2 Glyoxylate Cycle

The glyoxylate cycle bypasses the rate-limiting decarboxylation steps of the TCA cycle by utilizing 2 moles of acetyl-CoA and producing 1 mole of oxaloacetate and allowing the carbon atoms derived from fatty-acid oxidation to be converted to glucose.[5] In the past it was generally accepted that the glyoxylate cycle existed in microorganisms and higher plants but was absent in higher animals; however, there is data to support the conclusion that the activation of the

glyoxylate cycle can serve as a part of the mobilization of carbohydrates and lipids by adrenaline and that the fatty acids produced from fat not only maintain energy reactions, but gluconeogenesis as well.[6] Among the 5 enzymes that participate in this cycle, aconitase, citrate synthase and malate dehydrogenase are the enzymes common to the TCA cycle. Assays of these enzymes common to both the TCA and glyoxylate cycles show that their activities were 20-40% higher in the livers of newborn rats versus adult rats, perhaps suggesting an activation of the glyoxylate cycle as a result of adrenaline produced during the first few days after birth.[6]

1.3 Aconitase

Citrate, a key metabolite in the TCA cycle, is implicated in many processes such as inflammation, cancer, insulin secretion, histone acetylation and neurological disorders.[7] The greater understanding of the dual role of citrate in the survival and expansion of cancer has directed attention to two enzymes that determine the concentration and ultimate destination of citrate: citrate synthase (CS) and aconitase, with the focus of this work on aconitase. It has been shown that under iron rich conditions the isomerization of citrate to isocitrate is catalyzed in two steps by the enzyme aconitase in the TCA cycle as well as in the glyoxylate cycle. Aconitase first dehydrates citrate, removing the elements of water to yield aconitate, which is then rehydrated with H and OH added back in opposite positions to produce isocitrate. This allows for the TCA cycle to oxidize a newly secondary alcohol as opposed to directly oxidizing the tertiary alcohol.

The aconitase superfamily encompasses five phylogenetic groups: (i) mitochondrial aconitases (mAcn), (ii) cytoplasmic aconitases (cAcn) and iron regulatory proteins (IRP1 and IRP2) of

higher organisms and bacterial aconitase A's (AcnA), (iii)homoaconitases, (iv) fungal and bacterial isopropylmalate isomerases (IPMI), and (v) bacterial aconitase B's (AcnB).[8]

In the antibiotic producing species *Streptomyces viridochromogenes,* Tü494, sufficient iron present allows AcnA to function as this enzyme of the TCA cycle while insufficient iron results in AcnA functioning as a regulator of iron metabolism and oxidative stress response.[9] This is achieved by the iron-sulfur prosthetic group structure of aconitase, a cube-like cluster essential for activity.[10] Insufficient iron or oxidative stress causes the $[4Fe\text{-}4S]^{2+}$ catalytic center cluster to disassemble and reform to the catalytically inactive apo-enzyme [3Fe-4s]+ that is accessible for binding of iron response elements (IRE).[11] AcnA enzymes from *S. viridochromogenes* and *E. coli* as well as IRP1 in eukaryotes have been shown to serve in this bifunctional manner; they can serve not only as enzymes but also as post-transcriptional regulators.[12]

1.3.1 Isozymes of Aconitase

Many of the enzymes of the TCA cycle, including aconitase, are known to exist in both cytosolic and mitochondrial forms. Results of biochemical and phylogenetic studies suggest that early during the evolution of the aconitase family, a gene duplication enabled a cytosolic aconitase to evolve independently from the mitochondrial aconitase, and another duplication of the cytosolic aconitase resulted in two cytosolic homologues in animals that subsequently acquired the RNA binding capabilities of aconitase as mentioned above. Therefore, some unicellular eukaryotes and protozoan parasites contain single aconitase genes that encode isozymes with functions in the cytosol and the mitochondria meanwhile multicellular eukaryotes have separate genes that encode these isozymes.[13] For example, the cytosolic aconitase of *C. elegans* has no RNA-binding activity[14], while one of the two cytosolic aconitases in *Drosophila*

also functions as an RNA-binding, iron regulatory protein (IRP).[15] In mammals, IRP1 (also known as cytosolic aconitase, or ACO1) has both aconitase and RNA-binding functions, while IRP2 functions solely as a RNA-binding protein.[16]

The presence of two isozymes of aconitase in *E.coli* was first elucidated after the successful deletion of the *acnA* gene resulted in a mutant that still retained residual aconitase activity and did not demonstrate glutamate auxotrophy.[17] This provided evidence for the existence of 2 aconitases, designated AcnA and AcnB. The mutant and wild type aconitase both grew equally well under most growth conditions, demonstrating that the iron-sulfur isozymes are functionally overlapping; however, underlying functional specialization was suggested from the differential regulation of the genes under other growth conditions.[17]

In a study characterizing the stabilities of AcnA and AcnB, it was determined that under normal conditions, AcnB serves as the primary aconitase, processing the bulk of metabolic flux. [18] The same study determined that the enzyme AcnB is sensitive to both oxidative stress as well as iron depletion while AcnA on the other hand, is resistant to both stressors. During the early growth stage of *E.coli*, AcnB is the major aconitase expressed, while AcnA is expressed during the late growth stage.[19] This mechanism of differential expression of aconitase based on growth stage is useful for the organism to adapt to the necessities of the varying stages.

1.3.2 Aconitase Structure

As aforementioned, aconitase is an iron sulfur protein that utilizes an intact [4Fe-4S] to participate as an enzyme in the TCA cycle, while in some species in its disassembled apo-form it

can bind mRNA transcripts and serve as a posttranscriptional regulator. During cell growth, reactive oxygen species (ROS) such as peroxynitrite and hydrogen peroxide are accumulated in cells, causing damage and the subsequent inactivation of aconitase.[13] The oxidated, inactive, $[3Fe\text{-}4S]^{+}$ aconitase can be reactivated by intracellular iron and a reducing agent such as glutathione or cysteine. The amino acids of aconitase can also be targets of reactive species, resulting in nitrated, glutathionylated and carbonylated enzyme, among other potential modifications. The formation of disulfide or dityrosine bonds can also occur in this oxidated aconitase, resulting in aggregation of the protein. This oxidated $[3Fe\text{-}4S]^{+}$ form of aconitase is also susceptible to degradation by Lon Protease.[20]

The overall structures of *E.coli* and human aconitases are similar, despite having low sequence identities (**Figure 1.2**). In fact, when looking at equivalent residues of structues of mAcn and AcnB, it can be shown that 19 out of 23 active-site residues are identical, despite domain reorganization. The additional domain in AcnB has been characterized as a HEAT-like domain that has been found to form a tunnel leading to the aconitase active site, implicating this domain in protein-protein recognition and substrate channeling.[8]

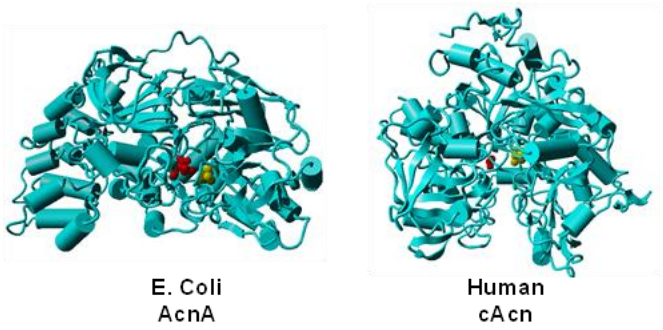

Figure 1.2. The structures of E. coli AcnB (PDB ID: 1I5J) and human cytosolic Acn (cAcn) (PDB ID: 2B3Y). The substrate isocitrate or aconitate was in red and Fe-S clusters are in yellow.

1.4 Post-translational Modifications

Simple proteins such as the enzyme ribonuclease and the contractile protein actin exist consisting of only amino acids with no other chemical groups. Other proteins, such as aconitase, exist containing various chemical constituents as an important part of their structure. These chemical constituents are brought about by modification of the primary structure or covalent alterations to the amino acid side chains after a protein has been synthesized. This is called post-translational modification. The four main groups of protein functions requiring covalent post-translational modifications of amino acid residue side chains are: (i) the necessity of a prosthetic group to be covalently bound to the polypeptide chain for activity of the enzyme, (ii) the switching on and off of enzyme activity, (iii) the intracellular localization of proteins and (iv) the spatial structure of the protein is influenced by such modification.[21] Post-translational modification of aconitase occurs in both redox-dependent and redox-independent manners, with the reversible oxidation of the iron-sulfur clusters and cysteine residues and the reversible phosphorylation being well-known mechanisms of posttranslational aconitase activity regulation.[22]

1.5 Acetylation/ Deacetylation

The reversible acetylation and deacetylation of lysine residues changes the positively charged epsilon-NH_3^+ group to a neutral amide. Proteomic studies show acetylation of metabolic enzymes as an important mechanism for regulation of metabolic substrates in metabolic pathways such as the TCA cycle.[1] The acetylation of lysine residues in the C-terminal domains of certain proteins has been found to have the capability to protect the protein from further modification that would decrease the lifespan or functioning time of the protein, thus increasing such factors.[23]

The enzymatic deacetylation of proteins is performed by a family of enzymes known as sirtuins. Sirtuin 3 (SIRT3) is a deacetylase present in the mitochondria that plays a primary role in regulation of mitochondrial acetylation. The deacetylation of lysine residues is catalyzed by protein lysine deacetylases (KDAC), with the sirtuin-type CobB being the well-known KDAC in *E. coli.*

The change of charge that acetylation brings allows cells to sense energy status and respond to environmental stimuli accordingly. Therefore, this modification results in activation for some enzymes while it results in inhibition of others. In human prostate adenocarcinoma, mitochondrial aconitase (ACO2) has been noted to have increased activity compared to adjacent normal tissue, with the acetylation of Lysine 258 being identified to play a regulatory role in the function of this enzyme.[18] Acetylation of ACO2 is reversibly regulated by SIRT3, with the reduction of SIRT3 leading ACO2 to exhibit the increased TCA cycle activity found in prostate cancer metastatic lesions. The acetylation of K144 in human heart mitochondrial aconitase has also been found to activate the enzyme *in vivo.*[25]

1.6 Genetic Code Expansion (GCE)

During protein synthesis, the ribosome translates mRNA sequences into polypeptides through the matching of complementary aminoacylated tRNAs with their triplet-codons. There are 3 triplet STOP codons (TAA, TGA and TAG, designated as "ochre," "opal" and "amber," respectively)[25] that trigger the release of the newly formed polypeptide chain from the ribosome, due to the absence of tRNAs with anticodons complementary to the STOP codons.

In this project, the genetic code expansion strategy is applied to homogeneously incorporate acetyllysine (AcK) at determined positions on the *E.coli* aconitase AcnA and AcnB isozymes and monitor the effects caused by the modification. This direct co-translational incorporation of modified amino acids is dependent upon three major premises: 1) the existence of an orthogonal aminoacyl-tRNA synthetase (aaRS)/tRNA pair, 2) specificity of the aaRS for an unnatural amino acid and 3) the presence of a "blank" codon.

As mentioned above, 3 triplet codons designated as STOP codons normally cause the termination of translation; however, in some species such as Archean *Methanococcus jannaschii* the amber codon is used to introduce an amino acid such as tyrosine at a UAG codon.[26] This has been used advantageously for recombinant expression of therapeutic proteins in *E. coli*, with the *Methanococcus jannaschii* derived TyrRS/$tRNA^{Tyr}$ pair (*Mj*TyrRS/$tRNA^{Tyr}$) being the most widely used aaRS/tRNA pair.[27] (**Figure 1.3**)

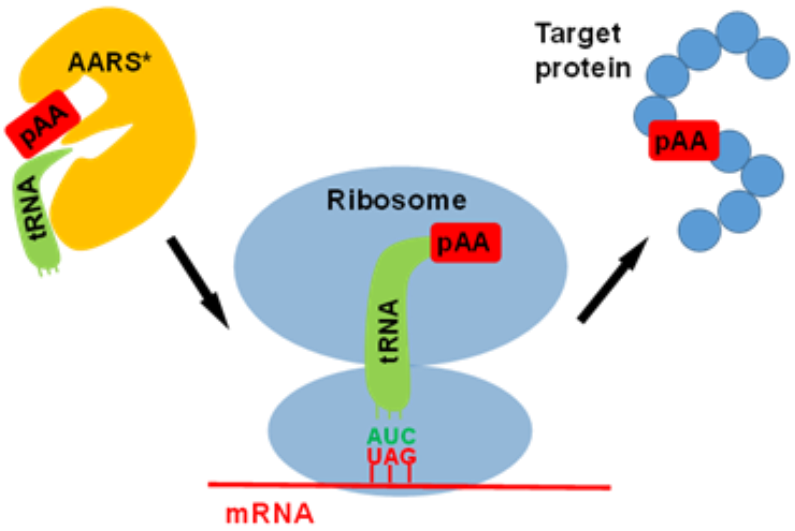

Figure 1.3. The strategy of genetic code expansion. The projected AA (pAA) is specifically recognized by an engineered aminoacyl-tRNA synthetase (AARS) and attached to an orthogonal tRNA, which is decoded on the ribosome during translation in response to an introduced stop codon, allowing the incorporation of pAA into the target protein at a controlled site.

1.7 References

1) Garrett, R. H.; Grisham, C. M. *Biochemistry*; Cengage, 2017.

(2) Akram, M. Citric Acid Cycle and Role of its Intermediates in Metabolism. *Cell Biochemistry and Biophysics* **2014**, *68* (3), 475-478, Review. DOI: 10.1007/s12013-013-9750-1.

(3) Kang, W.; Suzuki, M.; Saito, T.; Miyado, K. Emerging Role of TCA Cycle-Related Enzymes in Human Diseases. *International Journal of Molecular Sciences* **2021**, *22* (23), Article. DOI: 10.3390/ijms222313057.

(4) Munnich, A. Casting an eye on the Krebs cycle. *Nature Genetics* **2008**, *40* (10), 1148-1149, Editorial Material. DOI: 10.1038/ng1008-1148.

(5) KORNBERG, H.; KREBS, H. SYNTHESIS OF CELL CONSTITUENTS FROM C2-UNITS BY A MODIFIED TRICARBOXYLIC ACID CYCLE. *Nature* **1957**, *179* (4568), 988-991, Article. DOI: 10.1038/179988a0.

(6) Morgunov, I.; Kondrashova, M.; Kamzolova, S.; Sokolov, A.; Fedotcheva, N.; Finogenova, T. Evidence of the glyoxylate cycle in the liver of newborn rats. *Medical Science Monitor* **2005**, *11* (2), BR57-BR60, Article.

(7) Huang, L.; Wang, C.; Xu, H.; Peng, G. Targeting citrate as a novel therapeutic strategy in cancer treatment. *Biochimica Et Biophysica Acta-Reviews on Cancer* **2020**, *1873* (1), Review. DOI: 10.1016/j.bbcan.2019.188332.

(8) Williams, C.; Stillman, T.; Barynin, V.; Sedelnikova, S.; Tang, Y.; Green, J.; Guest, J.; Artymiuk, P. E-coli aconitase B structure reveals a HEAT-like domain with implications for protein-protein recognition. *Nature Structural Biology* **2002**, *9* (6), 447-452, Article. DOI: 10.1038/nsb801.

(9) Michta, E.; Schad, K.; Blin, K.; Ort-Winklbauer, R.; Rottig, M.; Kohlbacher, O.; Wohlleben, W.; Schinko, E.; Mast, Y. The bifunctional role of aconitase in Streptomyces viridochromogenes Tu494. *Environmental Microbiology* **2012**, *14* (12), 3203-3219, Article. DOI: 10.1111/1462-2920.12006.

(10) PRODROMOU, C.; HAYNES, M.; GUEST, J. THE ACONITASE OF ESCHERICHIA-COLI - PURIFICATION OF THE ENZYME AND MOLECULAR-CLONING AND MAP LOCATION OF THE GENE (ACN). *Journal of General Microbiology* **1991**, *137*, 2505-2515, Article. DOI: 10.1099/00221287-137-11-2505.

(11) Michta, E.; Ding, W.; Zhu, S. C.; Blin, K.; Ruan, H. Q.; Wang, R.; Wohlleben, W.; Mast, Y. Proteomic Approach to Reveal the Regulatory Function of Aconitase AcnA in Oxidative Stress Response in the Antibiotic Producer Streptomyces viridochromogenes Tu494. *Plos One* **2014**, *9* (2). DOI: 10.1371/journal.pone.0087905.

(12) Tang, Y.; Guest, J. Direct evidence for mRNA binding and post-transcriptional regulation by Escherichia coli aconitases. *Microbiology-Sgm* **1999**, *145*, 3069-3079, Article. DOI: 10.1099/00221287-145-11-3069.

(13) Castro, L.; Tortora, V.; Mansilla, S.; Radi, R. Aconitases: Non-redox Iron-Sulfur Proteins Sensitive to Reactive Species. *Accounts of Chemical Research* **2019**, *52* (9), 2609-2619, Review. DOI: 10.1021/acs.accounts.9b00150.

(14) Gourley, B.; Parker, S.; Jones, B.; Zumbrennen, K.; Leibold, E. Cytosolic aconitase and ferritin are regulated by iron in Caenorhabditis elegans. *Journal of Biological Chemistry* **2003**, *278* (5), 3227-3234, Article. DOI: 10.1074/jbc.M210333200.

(15) Lind, M.; Missirlis, F.; Melefors, O.; Uhrigshardt, H.; Kirby, K.; Phillips, J.; Soderhall, K.; Rouault, T. Of two cytosolic aconitases expressed in drosophila, only one functions as an iron-regulatory protein. *Journal of Biological Chemistry* **2006**, *281* (27), 18707-18714, Article. DOI: 10.1074/jbc.M603354200.

(16) Pantopoulos, K.; LeVine, S.; Connor, J.; Schipper, H. Iron metabolism and the IRIE/IRP regulatory system - An update. *Redox-Active Metals in Neurological Disorders* **2004**, *1012*, 1-13, Article. DOI: 10.1196/annals.1306.001.

(17) GRUER, M.; GUEST, J. 2 GENETICALLY-DISTINCT AND DIFFERENTIALLY-REGULATED ACONITASES (ACNA AND ACNB) IN ESCHERICHIA-COLI. *Microbiology-Sgm* **1994**, *140*, 2531-2541, Article. DOI: 10.1099/00221287-140-10-2531.

(18) Varghese, S.; Tang, Y.; Imlay, J. Contrasting sensitivities of Escherichia coli aconitases A and B to oxidation and iron depletion. *Journal of Bacteriology* **2003**, *185* (1), 221-230, Article. DOI: 10.1128/JB.185.1.221-230.2003.

(19) Cunningham, L.; Gruer, M.; Guest, J. Transcriptional regulation of the aconitase genes (acnA and acnB) of Escherichia coli. *Microbiology-Uk* **1997**, *143*, 3795-3805, Article. DOI: 10.1099/00221287-143-12-3795.

(20) Quirós, P. M. Determination of Aconitase Activity: A Substrate of the Mitochondrial Lon Protease. *Proteases and Cancer: Methods and Protocols, Methods in Molecular Biology* **2018**, *1731*, 49-56.

(21) Knorre, D.; Kudryashova, N.; Godovikova, T. Chemical and Functional Aspects of Posttranslational Modification of Proteins. *Acta Naturae* **2009**, *1* (3), 29-51, Review. DOI: 10.32607/20758251-2009-1-3-29-51.

(22) Lushchak, O.; Piroddi, M.; Galli, F.; Lushchak, V. Aconitase post-translational modification as a key in linkage between Krebs cycle, iron homeostasis, redox signaling, and metabolism of reactive oxygen species. *Redox Report* **2014**, *19* (1), 8-15, Review. DOI: 10.1179/1351000213Y.0000000073.

(23) Feng, L.; Lin, T.; Uranishi, H.; Gu, W.; Xu, Y. Functional analysis of the roles of posttranslational modifications at the p53 C terminus in regulating p53 stability and activity.

Molecular and Cellular Biology **2005**, *25* (13), 5389-5395, Article. DOI: 10.1128/MCB.25.13.5389-5395.2005.

(24) Dessai, A.; Dominguez, M.; Chen, U.; Hasper, J.; Prechtl, C.; Yu, C.; Katsuta, E.; Dai, T.; Zhu, B.; Jung, S.; et al. Transcriptional Repression of SIRT3 Potentiates Mitochondrial Aconitase Activation to Drive Aggressive Prostate Cancer to the Bone. *Cancer Research* **2021**, *81* (1), 50-63, Article. DOI: 10.1158/0008-5472.CAN-20-1708.

(25) Wals, K.; Ovaa, H. Unnatural amino acid incorporation in E. coli: current and future applications in the design of therapeutic proteins. *Frontiers in Chemistry* **2014**, *2*, Review. DOI: 10.3389/fchem.2014.00015.

(26) Huang, Y.; Liu, T. Therapeutic applications of genetic code expansion. *Synthetic and Systems Biotechnology* **2018**, *3* (3), 150-158, Review. DOI: 10.1016/j.synbio.2018.09.003.

CHAPTER 2

Studying acetylation of aconitase isozymes by genetic code expansion*

* This chapter was adapted from the original publication (Jessica Araujo, Sara Ottinger, Sumana Venkat, Qinglei Gan, Chenguang Fan*. Studying acetylation of aconitase isozymes by genetic code expansion. Front. Chem. 2022; 10:862483.)

2.1 Abstract

Aconitase catalyzes the second reaction of the tricarboxylic acid cycle, the reversible conversion of citrate and isocitrate. Escherichia coli has two isoforms of aconitase, AcnA and AcnB. Acetylomic studies have identified acetylation at multiple lysine sites of both E. coli aconitase isozymes, but the impacts of acetylation on aconitases are unknown. In this study, we applied the genetic code expansion approach to produce 14 site-specifically acetylated aconitase variants. Enzyme assays and kinetic analyses showed that acetylation of AcnA K684 decreased the enzyme activity, while acetylation of AcnB K567 increased the enzyme activity. Further in vitro acetylation and deacetylation assays were performed, which indicated that both aconitase isozymes could be acetylated by acetyl-phosphate chemically and be deacetylated by the CobB deacetylase at most lysine sites. Through this study, we have demonstrated practical applications of genetic code expansion in acetylation studies.

2.2 Introduction

Aconitase catalyzes the reversible conversion of citrate and isocitrate in the tricarboxylic acid (TCA) and glyoxylate cycles. It is an iron-sulfur (Fe-S) enzyme.[1] Depending on the state of the Fe-S cluster, aconitase has three forms: the active [4Fe-4S] form, the inactive [3Fe-4S] form, and

the apo-enzyme form. The [4Fe-4S] cluster is sensitive to reactive oxygen species (ROS) and iron depletion which impair aconitase activities, so aconitases are widely used as biomarkers for oxidative stress and intracellular sensors of iron and redox states.[2, 3] In E. coli cells, there are two aconitase isozymes, AcnA and AcnB.[4] Enzymological and regulatory analyses indicated that AcnB is the major TCA enzyme expressed during the exponential phase while AcnA is synthesized during the stationary phase or under stress conditions.[5] Inactivated by ROS or iron depletion, both AcnA and AcnB apo-enzymes can bind to 3'-untranslated region of acnA and acnB mRNAs to stabilize them and increase their own expression, mediating a post-transcriptional positive autoregulation.[6] Furthermore, aconitases are also regulated by post-translational modifications (PTMs), mostly oxidation, nitrosylation, and thiolation of cysteine residues around the Fe-S cluster.[7] Recently, a number of acetylated lysine residues have been identified in aconitase isozymes of both mammals and bacteria.[8] Two studies on human mitochondrial aconitase (mAcn) showed that acetylation of K144 and K258 can increase the enzyme activity.[9, 10] [10] However, both E. coli AcnA and AcnB have low sequence identities with human mAcn, so the impacts of acetylation on aconitase isozymes in E. coli remain unknown.

The classic approach to study lysine acetylation is to use glutamine (KQ mutation) as a mimic of acetyllysine. However, this method undermines the structural difference between glutamine and acetyllysine. The side chain of glutamine residue is ~4Å shorter than acetyllysine, so it may not reflect the real impacts of lysine acetylation. Indeed, our previous study on lysine acetylation of isocitrate dehydrogenase compared its activity with KQ mutations and real acetylated lysine residues, showing that at some acetylation sites the KQ mutation method derived different or even opposite conclusions.[11] To overcome this problem, the genetic code expansion technique

has been used to generate site-specifically acetylated enzyme variants. This technique introduces an aminoacyl-tRNA synthetase which has been engineered to recognize acetyllysine and a tRNA which can decode a stop codon (UAG) as acetyllysine to produce site-specifically and purely acetylated proteins.[12] In this work, we used this approach to study lysine acetylation of aconitase isozymes, demonstrating a practical application of genetic code expansion in protein PTM studies.

2.3 Materials and Methods

General molecular biology and protein analyses

Chemicals were purchased from VWR International (Radnor, PA, USA) or Chem-Impex International (Wood Dale, IL, USA). Plasmid were constructed by the NEBuilder HiFi DNA Assembly Kit (New England Biolabs, Ipswich, MA, USA). Point mutations were generated by the Q5 Site-Directed Mutagenesis Kit (New England Biolabs). For western blotting, purified aconitase isozymes and their variants were separated on SDS PAGE gels and transferred to the PVDF membranes. The horseradish peroxidase (HRP)-conjugated acetyllysine antibody (Cell Signaling Technology, Danvers, MA, USA) was used as the primary antibody, and chemiluminescence for detection was generated by Pierce ECL Western Blotting substrates (Thermo Scientific, Waltham, MA, USA).

Expression and purification of aconitases and acetylated variants

The gene of acnA or acnB or their mutants was cloned into the pCDF-1b plasmid (EMD Millipore, Burlington, MA, USA) with a C-terminal His6-tag, individually. Then it was transformed into BL21 (DE3) cells together with the acetyllysine incorporation system routinely

used in our group.[13] Cells was grown in 400 mL of LB medium with 100 μg/mL streptomycin, 50 μg/mL chloramphenicol, 10 mM acetyllysine, and 20 mM nicotinamine (NAM, the deacetylase inhibitor) at 37°C to OD 600nm of 0.6–0.8, then 0.1 mM Isopropyl β-D-1-thiogalactopyranoside (IPTG) was added to induce protein expression. Cells were then incubated at 16°C for an additional 12 h and harvested by centrifugation at 4,000 × g for 20 minutes at 4 °C. Cell pellets were suspended in 12 mL of 50 mM Tris (pH 7.8), 300 mM NaCl, 20 mM imidazole, 20 mM NAM, and 5 mM β-mercaptoethanol with cocktail protease inhibitors (Roche, Basel, Switzerland), and then broken by sonication. The crude extract was centrifuged at 20,000 × g for 30 min at 4°C. The soluble fraction was filtered through a 0.45-μm membrane and loaded onto a column containing 2 mL of Ni-NTA resin (Qiagen, Hilden, Germany). The column was then washed with 25 mL of 50 mM Tris (pH 7.8), 300 mM NaCl, 1mM DTT, and 50 mM imidazole, and eluted with 2 mL of 50 mM Tris (pH 7.8), 300 mM NaCl, 1mM DTT, and 200 mM imidazole. SDS-PAGE electrophoresis was performed to check the purity of aconitases and their variants. Western blotting and mass spectrometry were performed to confirm the incorporation of acetyllysine at correct sites.

The aconitase activity assay and kinetic analyses

Before enzyme activity assays, purified aconitases and their acetylated variants were reactivated by incubating with 1 mM (NH4)2Fe(SO4)2 and 5 mM DTT in 50 mM Tris (pH 8) for 30 minutes following previous protocols.[14] Enzyme assays were performed with the commercial aconitase assay kit from BioAssay System (Hayward, CA). Briefly, it measures the isocitrate generated as a product of the aconitase reaction. The isocitrate is then oxidized producing NADPH and the oxidation product. The NADPH converts the dye to an intense violet color with

an absorption maximum at 565 nm. The increase in absorbance at 565 nm is directly proportional to aconitase activity. To determine steady-state kinetic parameters, the concentration of the substrate citrate was varied from 0.1 mM to 50 mM. Kinetic parameters were calculated by non-liner regression with software Grafit (Erithacus Software).

Mass spectrometry (MS) analyses

The LC-MS/MS analyses were performed by the Yale Keck Proteomics facility and followed the previous protocol.[11] Briefly, aconitases and their variants were separated by SDS-PAGE electrophoresis. Protein bands were cut and digested in gel by trypsin, and analyzed by LC-MS/MS on an LTQ Orbitrap XL equipped with a nanoACQUITY UPLC system. The Mascot search algorithm was used to search for the substitution of the lysine residue with acetyllysine.

The in vitro acetylation assay

The acetylation reaction was performed in the buffer of 50 mM Tris (pH 8.0), 0.1 mM EDTA, 1 mM DTT and 10 mM sodium butyrate, initiated by mixing 10 μg enzyme and 3 mM AcP in a total volume of 100 μl, and then incubated at 37°C for 1 hour.

The in vitro deacetylation assay

The deacetylation reaction was performed in the buffer of 50 mM HEPES (pH 7.0), 5 mM MgCl2, 1.0 mM NAD+, and 1 mM DTT, initiated by mixing 10 μg enzyme and 10 μg purified CobB in a total volume of 100 μl, and then incubated at 37°C for 1 hour.

2.4 Results

Generation of site-specifically acetylated aconitase variants

Several quantitative acetylomic studies of E. coli cells have demonstrated that both aconitase isoenzymes have higher acetylation stoichiometry than many other E. coli proteins. [15] [16] [17] Thus, we aimed to identify the effects of acetylation on aconitase isoenzymes site-specifically. Although a series of acetylomic studies have been performed for E. coli cells, the sets of acetylation sites identified in aconitase isoenzymes do not overlap well because of differences in strains, growth media, and MS detection and resolutions.[18] [19] [20] [21] [22] [23] [24] [25] [26] To be feasible and avoid biased selection, we chose all the lysine residues identified to be acetylated by more than three independent acetylomic studies, which were K164, K342, K482, K684 of AcnA and K77, K373, K396, K407, K539, K559, K567, K728, K759, K835 of AcnB.

In this study, we utilized our optimized acetyllysine incorporation system to produce site-specifically acetylated aconitase variants at selected sites listed above individually.[13] To minimize the non-specific acetylation of other lysine residues in aconitases, we used the BL21 (DE3) strain as the host cell line, which has a low level of acetylation globally.[21] Our previous studies on acetylation of malate dehydrogenase, isocitrate dehydrogenase, and citrate synthase have shown that those wild-type enzymes purified from BL21 (DE3) cells have low levels of non-specific acetylation.[27] [11] [28] As expected, wild-type AcnA and AcnB overexpressed in BL21 (DE3) cells had no or very weak level of acetylation (Figure S1). We fused the His6-tag to the C-terminus of aconitase variants for easy purification and to remove truncated proteins terminated at inserted UAG codons. All the purified acetylated aconitase variants had clear single bands in SDS-PAGE gels and were detected by the acetyllysine antibody in western blots (Figure S1).

The positions of acetyllysine incorporation were confirmed by LC-MS/MS analyses (Figure S2-S15).

The site-specific effects of lysine acetylation on aconitase activities

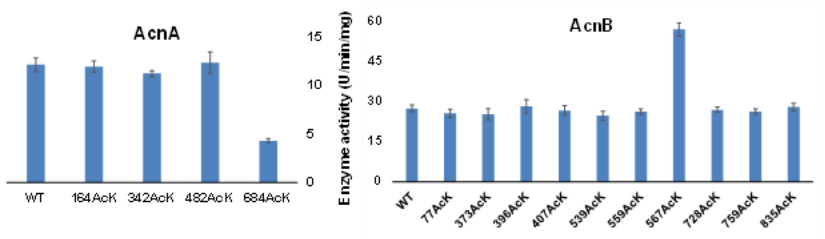

	K_M (mM)	k_{cat} (s^{-1})	k_{cat}/K_M (s^{-1} mM^{-1})
WT AcnA	1.64 ± 0.21	20.6 ± 1.62	12.6
AcnA-684AcK	3.45 ± 0.23	7.33 ± 0.89	2.1
WT AcnB	9.34 ± 0.72	63.5 ± 4.52	6.8
AcnB-567AcK	9.76 ± 0.67	125 ± 9.32	12.8

First, we measured the enzyme activities of purified AcnA and AcnB as well as their site-specifically acetylated variants with the commercial kit individually **(Figure 2.1).** Acetylation of most lysine sites had no significant effects on aconitase activities. There were only two variants which significantly affect aconitase activities. Interestingly, the impacts of acetylation on enzyme activities were different in aconitase isozymes. Acetylation of AcnA K684 decreased the activity by ~3-fold while acetylation of AcnB K567 increased the activity by ~2-fold.

Figure 2.1. The enzyme activities and kinetic analyses of AcnA, AcnB and their acetylated variants. The upper panel is enzyme activities measured by the commercial kit with 50 mM citrate as the substrate concentration. Mean values and standard deviations were calculated based on three replicates. The lower panel is the steady-state kinetic parameters. Kinetic parameters were calculated by non-liner regression with software Grafit.

To obtain insights into the impacts of acetylation on aconitase activities, we performed steady-state kinetic analyses of AcnA and AcnB as well as those two variants (AcnA-684AcK and AcnB-567AcK) which significantly affected activities. Acetylation of AcnA K684 impairs both the substrate binding and the turnover number while acetylation of AcnB K567 only enhances the turnover number.

The acetyl-phosphate-dependent acetylation of aconitase isozymes

It is known that lysine acetylation in E. coli is mostly generated non-enzymatically with acetyl-phosphate (AcP) as the acetyl-donor while acetyl-CoA-dependent enzymatic acetylation only applies for a small portion of proteins.[21] [29] Our previous studies also showed that AcP itself can acetylate several TCA cycle enzymes chemically.[11] [28] In this study, WT AcnA and AcnB expressed in BL21 (DE3) cells were purified and treated with 3 mM AcP in vitro. Western blots showed that AcP acetylated both AcnA and AcnB in a time-dependent manner (**Figure 2.2A**). The activities of AcnA and AcnB before and after AcP-treatment were measured. Consistent with site-specific results above, acetylation of AcnA impaired its activity while acetylation of AcnB enhanced its activity (**Figure 2.2B**). The impacts of acetylation by AcP-treatment were not as significant as the site-specific acetylation above, probably because AcP cannot acetylate lysine residues completely while purely acetylated variants were tested in above site-specific experiments.

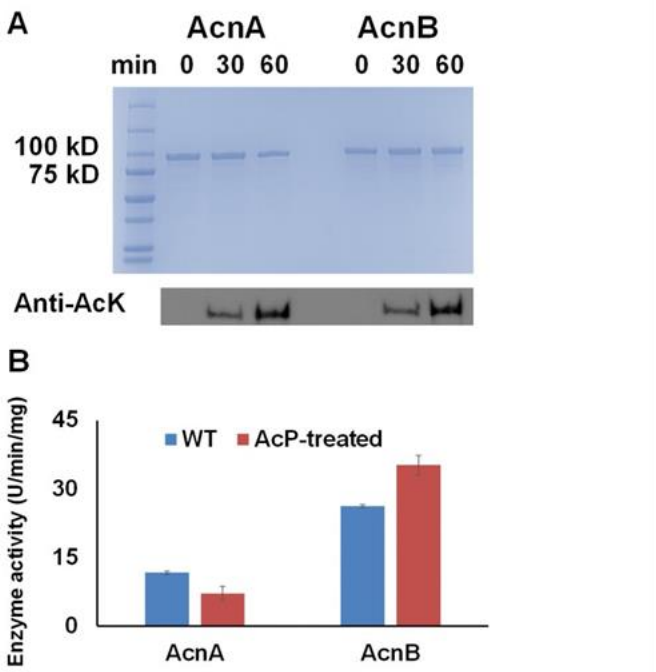

Figure 2.2. AcP-dependent acetylation of AcnA and AcnB. (A) SDS-PAGE and western blots of purified WT AcnA and WT AcnB treated with AcP in vitro. 2 μg of proteins were loaded for each lane. The full image of western blots is in Figure S16. (B) Enzyme activities of purified WT AcnA and WT AcnB before and after AcP-treatment. Mean values and standard deviations were calculated based on three replicates.

Then we performed LC-MS/MS analyses to identify acetylation sites in AcnA and AcnB by AcP-treatment. Those 14 sites selected for site-specific tests above were all acetylated by in vitro AcP-treatment. Besides them, we also identified 12 additional acetylation sites in AcnA (K10, K16, K116, K257, K283, K391, K406, K453, K578, K758, K770, and, K823) and 11 additional acetylation sites in AcnB (K20, K64, K73, K135, K137, K144, K356, K387, K571, K613, and K722). Among them, K116, K257, K406, K453, K578, K823 of AcnA and K64, K137 of AcnB

have not been identified to be acetylated in E. coli cells ever before, probably because acetylation of these sites has low stoichiometry and can be deacetylated easily in living cells. On the other hand, K18, K30, K71, K161, K460, K585, K832 of AcnA and K85, K110, K117, K221, K229, K267, K537, K588 of AcnB listed in the E. coli acetylation database[8] were not identified in our in vitro AcP-acetylation tests, implying that specific acetyltransferases or cofactors could be necessary for acetylation of these lysine sites in cells.

The CobB-dependent deacetylation of aconitase isozymes

Acetylation of lysine residues is reversible, and the deacetylation of acetylated lysine residues is catalyzed by protein lysine deacetylases (KDAC). To date, CobB is still the only well-known KDAC in E. coli.[30] Our previous studies showed that CobB can deacetylate acetylated lysine residues in several TCA cycle enzymes, but not for all the acetylation sites. In this study, we incubated those 14 site-specifically acetylated AcnA and AcnB variants with CobB, and used western blotting to determine the site specificity of CobB for AcnA and AcnB (**Figure 2.3A**). Most of acetylation sites were sensitive to CobB, while K164 of AcnA and K567, K728, K759 of AcnB were resistant to CobB.

Then we incubated AcP-treated AcnA and AcnB with CobB in vitro. After that, we measured the enzyme activities (**Figure 2.3B**). CobB-dependent acetylation restored AcnA activity but did not affect AcnB activity significantly. Acetylation of K684 in AcnA decreases AcnA activity and K684 is sensitive to CobB, so deacetylation of K684 could restore its enzyme activity. On the other hand, acetylation of K567 in AcnB increases AcnB activity but K567 is resistant to CobB, so CobB-dependent deacetylation could not restore AcnB activity. These results also indicated

that K684 of AcnA and K567 of AcnB are the two lysine residues whose acetylation affects their enzyme activities the most, which is consistent to our site-specific results above.

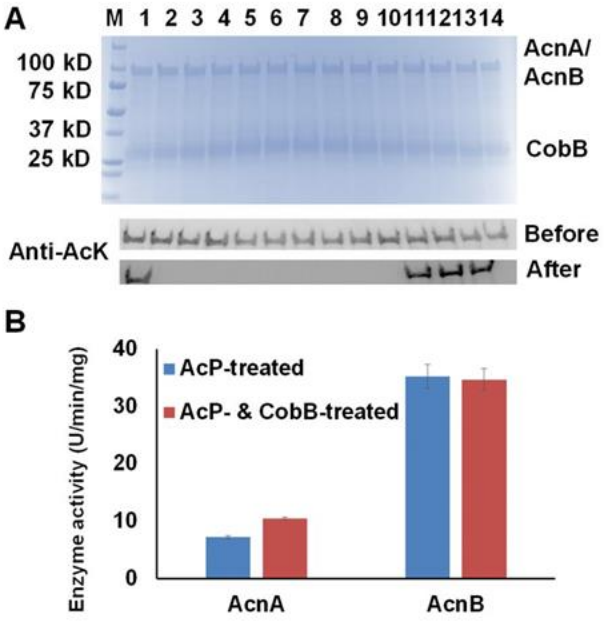

Figure 2.3. CobB-catalyzed deacetylation of AcnA and AcnB. (A) SDS-PAGE and western blots of site-specifically acetylated AcnA and AcnB variants incubated with CobB in vitro. 2 μg of AcnA/AcnB and CobB were loaded for each lane. The full image of western blots is in Figure S17. Samples from lane 1 to 4 are AcnA-164AcK, -342AcK, -482AcK, and -684AcK. Samples from lane 5 to 14 are AcnB-77AcK, 373-AcK, -396AcK, -407AcK, -539AcK, -559AcK, -567AcK, -728AcK, -759AcK, and -835AcK. (B) Enzyme activities of AcP-treated AcnA and AcnB before and after CobB-incubation. Mean values and standard deviations were calculated based on three replicates.

2.5 Discussion

The effects of acetylation on aconitase activities

Before our work, only two papers have reported acetylation of aconitase isoenzymes, which showed that acetylation of K144 and K258 in human mAcn activates enzyme activities.[9, 10] To find the structure-function relationships of aconitase acetylation, we mapped those two lysine residues onto the crystal structures of mAcn. Because there is no reported human mAcn structures, we used bovine mAcn as the model which has 96% sequence identify with human mAcn (**Figure 2.4A**). The active site is at the center of the enzyme (the purple molecule is the intermediate analog methyl-isocitrate). K144 is at the back of the active site. The previous study proposed that acetylation of K144 strengthens its interaction with the nearby Q541, hence inducing conformational changes to facilitate substrate binding.[9] K258 is at the entrance of the active site, so its acetylation could also cause conformational changes to enhance enzyme activities.

Although both E. coli AcnA and AcnB have low sequence identifies with human mAcn (28% and 24%, respectively), the overall structures of difference aconitases are very similar.[31] Thus, we mapped K684 of AcnA and K567 of AcnB onto their structures. The structure of human cytosolic Acn (cAcn) which has a 53% sequence identify with E. coli AcnA was used as the template for homology modeling for AcnA (**Figure 2.4B**). The structure of E. coli AcnB has been solved (**Figure 2.4C**). Clearly, both K684 of AcnA and K567 of AcnB are located at the entrance of the active sites of aconitase isozymes, like the position of K258 of human mAcn. However, the effects of acetylation of those two lysine residues are opposite. Similar to that of

K258 of human mAcn, acetylation of K567 of AcnB enhances the enzyme activity. On the other hand, acetylation of K684 of AcnA decreased the enzyme activity.

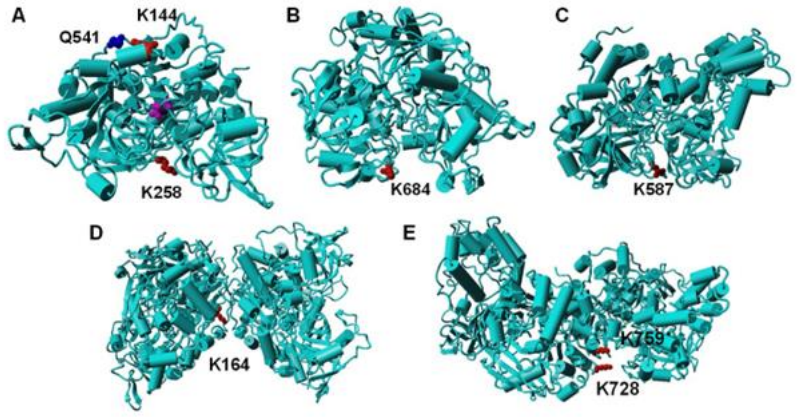

Figure 2.4. Mapping of acetylated lysine residues on the structures of AcnA and AcnB. A) The crystal structure of human cAcn (PDB ID: 2B3Y). B) The homology model of AcnA structure based on human cAcn. C) The crystal structure of AcnB (PDB ID: 1L5J). D) The homology model of AcnA dimer based on human cAcn. E) The dimer of AcnB (PDB ID: 1L5J).

Why do the same PTMs have totally opposite impacts on aconitase isozyme activities? We proposed that cells use this mechanism to adapt to different growth stages. E. coli. AcnB is the major aconitase which is expressed during the early growth stage.[5] During cell growth, ROS is accumulated in cells which damages aconitase.[3] In order to restore aconitase activities to maintain the necessary rate of the TCA cycle, cells use acetylation of AcnB to enhance its activity. During the late growth stage, AcnA is expressed.[5] Acetylation of AcnA decreases the enzyme activity, which is consistent with the slower metabolic rate in late growth stage.

The sensitivities of acetylated lysine residues in aconitases towards CobB deacetylase

Our deacetylation tests showed that CobB can remove most of acetylated lysine resides in both AcnA and AcnB (Figure 2.3). Then we mapped those residues which are sensitive to CobB (Figure S18). CobB-sensitive sites are all located at protein surface for easy CobB access, consistent with our previous studies on other TCA cycle enzymes.[11, 27] [28] On the other hand, we also mapped those residues which are resistant to CobB. Both AcnA and AcnB form dimers in solutions.[32] We used human cAcn as the template to model the AcnA structure. K164 of AcnA is located at the interface of two subunits (**Figure 2.4D**). K728 and K759 of AcnB are also at the subunit interface (**Figure 2.4E**). Such steric hindrance limits the access of CobB for deacetylation. Although K567 is located at the entrance of the active site, the primary amine group points to interior of the active site (**Figure 2.4C**), and this orientation also limits the access of CobB for deacetylation.

2.6 References

(1) Beinert, H.; Kennedy, M.; Stout, C. Aconitase as iron-sulfur protein, enzyme, and iron-regulatory protein. *Chemical Reviews* **1996**, *96* (7), 2335-2373, Review. DOI: 10.1021/cr950040z.

(2) Gardner, P. Aconitase: Sensitive target and measure of superoxide. *Superoxide Dismutase* **2002**, *349*, 9-23, Review. DOI: 10.1016/S0076-6879(02)49317-2.

(3) Castro, L.; Tortora, V.; Mansilla, S.; Radi, R. Aconitases: Non-redox Iron-Sulfur Proteins Sensitive to Reactive Species. *Accounts of Chemical Research* **2019**, *52* (9), 2609-2619, Review. DOI: 10.1021/acs.accounts.9b00150.

(4) GRUER, M.; GUEST, J. 2 GENETICALLY-DISTINCT AND DIFFERENTIALLY-REGULATED ACONITASES (ACNA AND ACNB) IN ESCHERICHIA-COLI. *Microbiology-Sgm* **1994**, *140*, 2531-2541, Article. DOI: 10.1099/00221287-140-10-2531.

(5) Cunningham, L.; Gruer, M.; Guest, J. Transcriptional regulation of the aconitase genes (acnA and acnB) of Escherichia coli. *Microbiology-Uk* **1997**, *143*, 3795-3805, Article. DOI: 10.1099/00221287-143-12-3795.

(6) Tang, Y.; Guest, J. Direct evidence for mRNA binding and post-transcriptional regulation by Escherichia coli aconitases. *Microbiology-Sgm* **1999**, *145*, 3069-3079, Article. DOI: 10.1099/00221287-145-11-3069.

(7) Lushchak, O.; Piroddi, M.; Galli, F.; Lushchak, V. Aconitase post-translational modification as a key in linkage between Krebs cycle, iron homeostasis, redox signaling, and metabolism of reactive oxygen species. *Redox Report* **2014**, *19* (1), 8-15, Review. DOI: 10.1179/1351000213Y.0000000073.

(8) Xu, H.; Zhou, J.; Lin, S.; Deng, W.; Zhang, Y.; Xue, Y. PLMD: An updated data resource of protein lysine modifications. *Journal of Genetics and Genomics* **2017**, *44* (5), 243-250, Article. DOI: 10.1016/j.jgg.2017.03.007.

(9) Fernandes, J.; Weddle, A.; Kinter, C.; Humphries, K.; Mather, T.; Szweda, L.; Kinter, M. Lysine Acetylation Activates Mitochondrial Aconitase in the Heart. *Biochemistry* **2015**, *54* (25), 4008-4018, Article. DOI: 10.1021/acs.biochem.5b00375.

(10) Dessai, A.; Dominguez, M.; Chen, U.; Hasper, J.; Prechtl, C.; Yu, C.; Katsuta, E.; Dai, T.; Zhu, B.; Jung, S.; et al. Transcriptional Repression of SIRT3 Potentiates Mitochondrial Aconitase Activation to Drive Aggressive Prostate Cancer to the Bone. *Cancer Research* **2021**, *81* (1), 50-63, Article. DOI: 10.1158/0008-5472.CAN-20-1708.

(11) Venkat, S.; Chen, H.; Stahman, A.; Hudson, D.; McGuire, P.; Gan, Q.; Fan, C. Characterizing Lysine Acetylation of Isocitrate Dehydrogenase in Escherichia coli. *Journal of Molecular Biology* **2018**, *430* (13), 1901-1911, Article. DOI: 10.1016/j.jmb.2018.04.031.

(12) Neumann, H.; Hancock, S.; Buning, R.; Routh, A.; Chapman, L.; Somers, J.; Owen-Hughes, T.; van Noort, J.; Rhodes, D.; Chin, J. A Method for Genetically Installing Site-Specific Acetylation in Recombinant Histories Defines the Effects of H3 K56 Acetylation. *Molecular Cell* **2009**, *36* (1), 153-163, Article. DOI: 10.1016/j.molcel.2009.07.027.

(13) Venkat, S.; Gregory, C.; Meng, K.; Gan, Q.; Fan, C. A Facile Protocol to Generate Site-Specifically Acetylated Proteins in Escherichia Coli. *Jove-Journal of Visualized Experiments* **2017**, (130), Article. DOI: 10.3791/57061.

(14) Bradbury, A.; Gruer, M.; Rudd, K.; Guest, J. The second aconitase (AcnB) of Escherichia coli. *Microbiology-Sgm* **1996**, *142*, 389-400, Article. DOI: 10.1099/13500872-142-2-389.

(15) Baeza, J.; Dowell, J.; Smallegan, M.; Fan, J.; Amador-Noguez, D.; Khan, Z.; Denu, J. Stoichiometry of Site-specific Lysine Acetylation in an Entire Proteome. *Journal of Biological Chemistry* **2014**, *289* (31), 21326-21338, Article. DOI: 10.1074/jbc.M114.581843.

(16) Meyer, J.; D'Souza, A.; Sorensen, D.; Rardin, M.; Wolfe, A.; Gibson, B.; Schilling, B. Quantification of Lysine Acetylation and Succinylation Stoichiometry in Proteins Using Mass Spectrometric Data-Independent Acquisitions (SWATH). *Journal of the American Society For Mass Spectrometry* **2016**, *27* (11), 1758-1771, Article. DOI: 10.1007/s13361-016-1476-z.

(17) Weinert, B.; Satpathy, S.; Hansen, B.; Lyon, D.; Jensen, L.; Choudhary, C. Accurate Quantification of Site-specific Acetylation Stoichiometry Reveals the Impact of Sirtuin Deacetylase CobB on the E-coli Acetylome. *Molecular & Cellular Proteomics* **2017**, *16* (5), 759-769, Article. DOI: 10.1074/mcp.M117.067587.

(18) Yu, B.; Kim, J.; Moon, J.; Ryu, S.; Pan, J. The diversity of lysine-acetylated proteins in Escherichia coli. *Journal of Microbiology and Biotechnology* **2008**, *18* (9), 1529-1536, Article.

(19) Zhang, J.; Sprung, R.; Pei, J.; Tan, X.; Kim, S.; Zhu, H.; Liu, C.; Grishin, N.; Zhao, Y. Lysine Acetylation Is a Highly Abundant and Evolutionarily Conserved Modification in Escherichia Coli. *Molecular & Cellular Proteomics* **2009**, *8* (2), 215-225, Article. DOI: 10.1074/mcp.M800187-MCP200.

(20) Colak, G.; Xie, Z.; Zhu, A.; Dai, L.; Lu, Z.; Zhang, Y.; Wan, X.; Chen, Y.; Cha, Y.; Lin, H.; et al. Identification of Lysine Succinylation Substrates and the Succinylation Regulatory Enzyme CobB in Escherichia coli. *Molecular & Cellular Proteomics* **2013**, *12* (12), 3509-3520, Article. DOI: 10.1074/mcp.M113.031567.

(21) Weinert, B.; Iesmantavicius, V.; Wagner, S.; Scholz, C.; Gummesson, B.; Beli, P.; Nystrom, T.; Choudhary, C. Acetyl-Phosphate Is a Critical Determinant of Lysine Acetylation in E. coli. *Molecular Cell* **2013**, *51* (2), 265-272, Article. DOI: 10.1016/j.molcel.2013.06.003.

(22) Zhang, K.; Zheng, S.; Yang, J.; Chen, Y.; Cheng, Z. Comprehensive Profiling of Protein Lysine Acetylation in Escherichia coli. *Journal of Proteome Research* **2013**, *12* (2), 844-851, Article. DOI: 10.1021/pr300912q.

(23) Castano-Cerezo, S.; Bernal, V.; Post, H.; Fuhrer, T.; Cappadona, S.; Sanchez-Diaz, N.; Sauer, U.; Heck, A.; Altelaar, A.; Canovas, M. Protein acetylation affects acetate metabolism, motility and acid stress response in Escherichia coli. *Molecular Systems Biology* **2014**, *10* (11), Article. DOI: 10.15252/msb.20145227.

(24) Kuhn, M.; Zemaitaitis, B.; Hu, L.; Sahu, A.; Sorensen, D.; Minasov, G.; Lima, B.; Scholle, M.; Mrksich, M.; Anderson, W.; et al. Structural, Kinetic and Proteomic Characterization of Acetyl Phosphate-Dependent Bacterial Protein Acetylation. *Plos One* **2014**, *9* (4), Article. DOI: 10.1371/journal.pone.0094816.

(25) AbouElfetouh, A.; Kuhn, M.; Hu, L.; Scholle, M.; Sorensen, D.; Sahu, A.; Becher, D.; Antelmann, H.; Mrksich, M.; Anderson, W.; et al. The E. coli sirtuin CobB shows no preference for enzymatic and nonenzymatic lysine acetylation substrate sites. *Microbiologyopen* **2015**, *4* (1), 66-83, Article. DOI: 10.1002/mbo3.223.

(26) Schilling, B.; Christensen, D.; Davis, R.; Sahu, A.; Hu, L.; Walker-Peddakotla, A.; Sorensen, D.; Zemaitaitis, B.; Gibson, B.; Wolfe, A. Protein acetylation dynamics in response to carbon overflow in Escherichia coli. *Molecular Microbiology* **2015**, *98* (5), 847-863, Article. DOI: 10.1111/mmi.13161.

(27) Venkat, S.; Gregory, C.; Sturges, J.; Gan, Q.; Fan, C. Studying the Lysine Acetylation of Malate Dehydrogenase. *Journal of Molecular Biology* **2017**, *429* (9), 1396-1405, Article. DOI: 10.1016/j.jmb.2017.03.027.

(28) Venkat, S.; Chen, H.; McGuire, P.; Stahman, A.; Gan, Q.; Fan, C. Characterizing lysine acetylation of Escherichia coli type II citrate synthase. *Febs Journal* **2019**, *286* (14), 2799-2808, Article. DOI: 10.1111/febs.14845.

(29) Hentchel, K.; Escalante-Semerena, J. Acylation of Biomolecules in Prokaryotes: a Widespread Strategy for the Control of Biological Function and Metabolic Stress. *Microbiology and Molecular Biology Reviews* **2015**, *79* (3), 321-346, Review. DOI: 10.1128/MMBR.00020-15.

(30) Starai, V.; Celic, I.; Cole, R.; Boeke, J.; Escalante-Semerena, J. Sir2-dependent activation of acetyl-CoA synthetase by deacetylation of active lysine. *Science* **2002**, *298* (5602), 2390-2392, Article. DOI: 10.1126/science.1077650.

(31) Williams, C.; Stillman, T.; Barynin, V.; Sedelnikova, S.; Tang, Y.; Green, J.; Guest, J.; Artymiuk, P. E-coli aconitase B structure reveals a HEAT-like domain with implications for protein-protein recognition. *Nature Structural Biology* **2002**, *9* (6), 447-452, Article. DOI: 10.1038/nsb801.

(32) Jordan, P.; Tang, Y.; Bradbury, A.; Thomson, A.; Guest, J. Biochemical and spectroscopic characterization of Escherichia coli aconitases (AcnA and AcnB). *Biochemical Journal* **1999**, *344*, 739-746, Article. DOI: 10.1042/0264-6021:3440739.

CHAPTER 3

3.1 Conclusion

The importance of the TCA cycle has been a process repeatedly highlighted in vital processes of life. The enzymes of the TCA cycle, which can exist in different modifiable forms, are functional to other pathways or can serve a non-enzymatic function. Further implicating the cycle in other processes, the metabolites of the TCA cycle can be useful in cell signaling. Aconitase is an iron-sulfur enzyme that catalyzes the isomerization of citrate to isocitrate in the TCA cycle under conditions of sufficient iron; however in some species its low iron, disassembled, apo-form it can bind mRNA transcripts to serve as a post-transcriptional regulator. It also participates in the glyoxylate cycle and its substrate, citrate, has been implicated in many disease states.

The focus of this research is to elucidate the effects of acetylation on the enzyme activity of the TCA cycle enzyme aconitase. The aconitase isozymes AcnA and AcnB in *E. coli* were acetylated at specific lysine residues and then the enzyme activity was determined. Utilizing Genetic Code Expansion, it was found that K567 of AcnB and K684 of AcnA are important residues with a potential role in the regulation of the isozymes during different growth stages.

3.2 Significance of this work

Acetylation of aconitase residues have been implicated in the regulation of the enzyme's activities in human mAcn, and with residue mapping on homology modeled structures it can reasonably be speculated that conserved residues are present in *E. coli*, thus illustrating the utility of this research for future understanding of TCA cycle isozyme structure-function relationship.

A greater understanding of the TCA cycle would greatly aid in the advancement of many fields of research. Metabolic dysregulation is a hallmark of cancer progression; however, much is unknown about the cellular processes that promote these metabolic alterations that drive metastatic cancer. The functioning of this centrally located pathway can determine life or death for an organism and thus, the research to reveal the inner workings of the enzymes involved is very valuable. The understanding of the mechanism by which various isozymes of the TCA cycle function within an organism must be fully understood in order to further the development of diagnostic, prognostic, and therapeutic techniques.

3.3 Future Directions

With improved methods available to aid in the study of protein modifications, the expansion of knowledge on acetylation in eukaryotes will indubitably prove to be useful. Future studies must be performed to validate the importance of these residues, *in vivo,* as modification can occur in a dynamic manner.

Supplementary Data

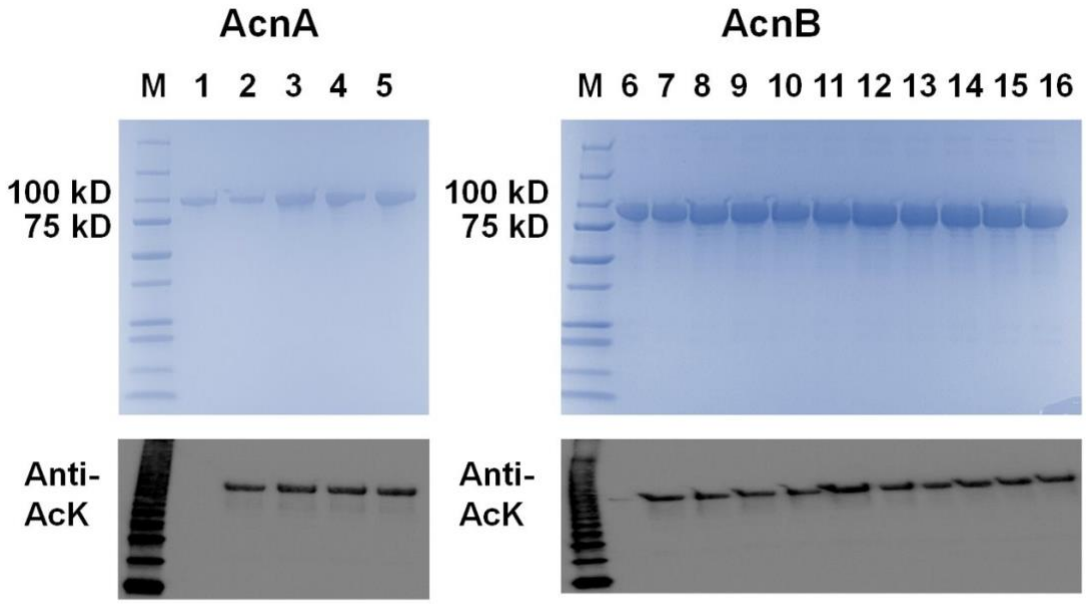

Figure S1. The incorporation of acetyllysine (AcK) at individual lysine sites of AcnA and AcnB. SDS-PAGE (upper panels) and western blots (lower panels) of purified aconitases and their variants from BL21(DE3) cells. Lane 1, wild-type AcnA; lane 2, AcnA-164AcK; lane 3, AcnA-342AcK; lane 4, AcnA-482AcK; lane 5; AcnA-684AcK; lane 6, wild-type AcnB; lane 7, AcnB-77AcK; lane 8, AcnB-373AcK; lane 9, AcnB-396AcK; lane 10, AcnB-407AcK; lane 11, AcnB-539AcK; lane 12, AcnB-559AcK; lane 13, AcnB-567AcK; lane 14, AcnB-728AcK; lane 15, AcnB-758AcK; lane 16, AcnB-835AcK. For each lane, 2 mg of purified proteins were loaded. Anti-AcK: acetyllysine antibody.

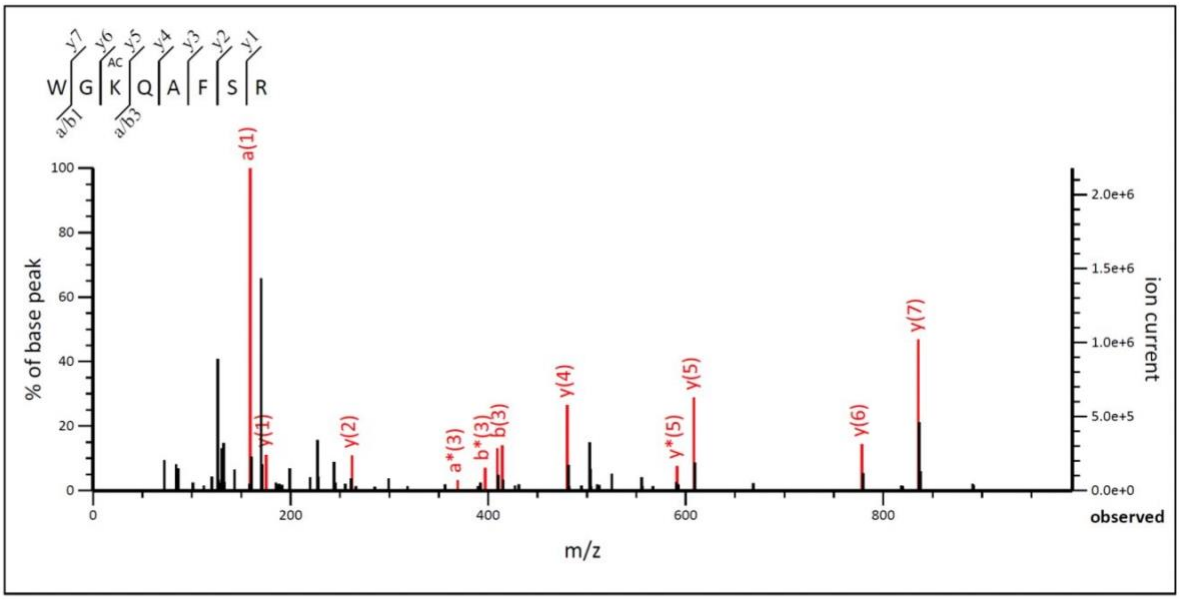

#	a	a^{++}	a*	a^{*++}	b	b^{++}	b*	b^{*++}	Seq.	y	y^{++}	y*	y^{*++}	#
1	**159.0917**	80.0495			187.0866	94.0469			W					8
2	216.1131	108.5602			244.1081	122.5577			G	***835.4421***	418.2247	818.4155	409.7114	7
3	386.2187	193.6130	369.1921	185.0997	**414.2136**	207.6104	397.1870	199.0972	K	***778.4206***	389.7139	761.3941	381.2007	6
4	514.2772	257.6423	497.2507	249.1290	542.2722	271.6397	525.2456	263.1264	Q	***608.3151***	304.6612	591.2885	296.1479	5
5	585.3144	293.1608	568.2878	284.6475	613.3093	307.1583	596.2827	298.6450	A	***480.2565***	240.6319	463.2300	232.1186	4
6	732.3828	366.6950	715.3562	358.1817	760.3777	380.6925	743.3511	372.1792	F	***409.2194***	205.1133	392.1928	196.6001	3
7	819.4148	410.2110	802.3883	401.6978	847.4097	424.2085	830.3832	415.6952	S	***262.1510***	131.5791	245.1244	123.0659	2
8									R	***175.1190***	88.0631	158.0924	79.5498	1

Figure S2. LC-MS/MS analysis of AcnA 164-AcK. The tandem mass spectrum of the peptide (residues 162-169) WGKQAFSR from purified AcnA 164-AcK. KAC denotes AcK incorporation. The partial sequence of the peptide containing the AcK can be read from the annotated a/b or y ion series. Matched peaks are in red.

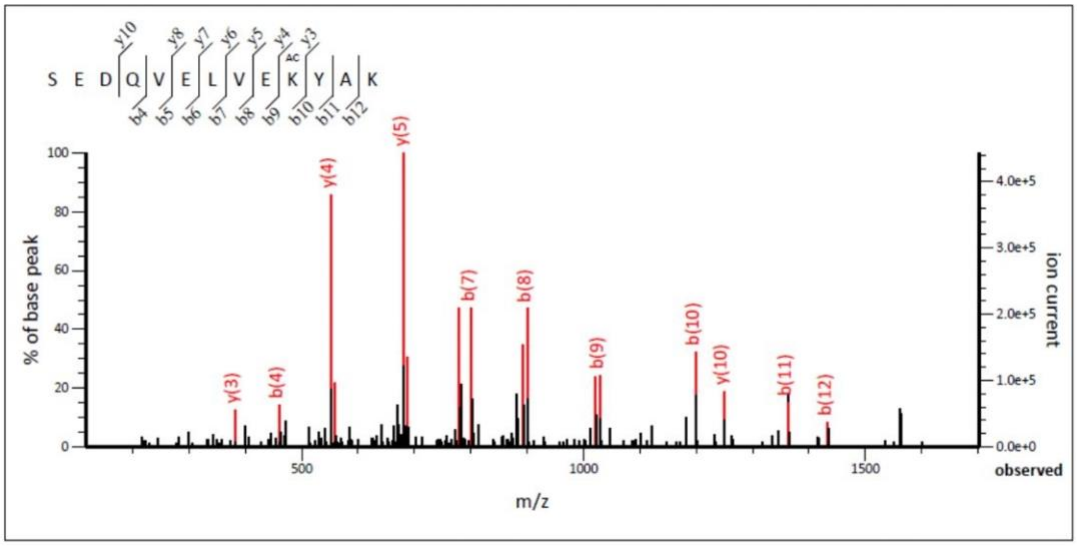

#	a	a*	b	b*	Seq.	y	y*	#
1	60.0444		88.0393		S			13
2	189.0870		217.0819		E	1492.7530	1475.7264	12
3	304.1139		332.1088		D	1363.7104	1346.6838	11
4	432.1725	415.1460	*460.1674*	443.1409	Q	**1248.6834**	1231.6569	10
5	531.2409	514.2144	*559.2358*	542.2093	V	1120.6249	1103.5983	9
6	660.2835	643.2570	*688.2784*	671.2519	E	**1021.5564**	1004.5299	8
7	773.3676	756.3410	*801.3625*	784.3359	L	**892.5138**	875.4873	7
8	872.4360	855.4094	*900.4309*	883.4044	V	**779.4298**	762.4032	6
9	1001.4786	984.4520	*1029.4735*	1012.4469	E	**680.3614**	663.3348	5
10	1171.5841	1154.5576	*1199.5790*	1182.5525	K	**551.3188**	534.2922	4
11	1334.6474	1317.6209	*1362.6424*	1345.6158	Y	**381.2132**	364.1867	3
12	1405.6846	1388.6580	*1433.6795*	1416.6529	A	218.1499	201.1234	2
13					K	147.1128	130.0863	1

Figure S3. LC-MS/MS analysis of AcnA 342-AcK. The tandem mass spectrum of the peptide (residues 333-345) SEDQVELVEKYAK from purified AcnA 342-AcK. KAC denotes AcK incorporation. The partial sequence of the peptide containing the AcK can be read from the annotated a/b or y ion series. Matched peaks are in red.

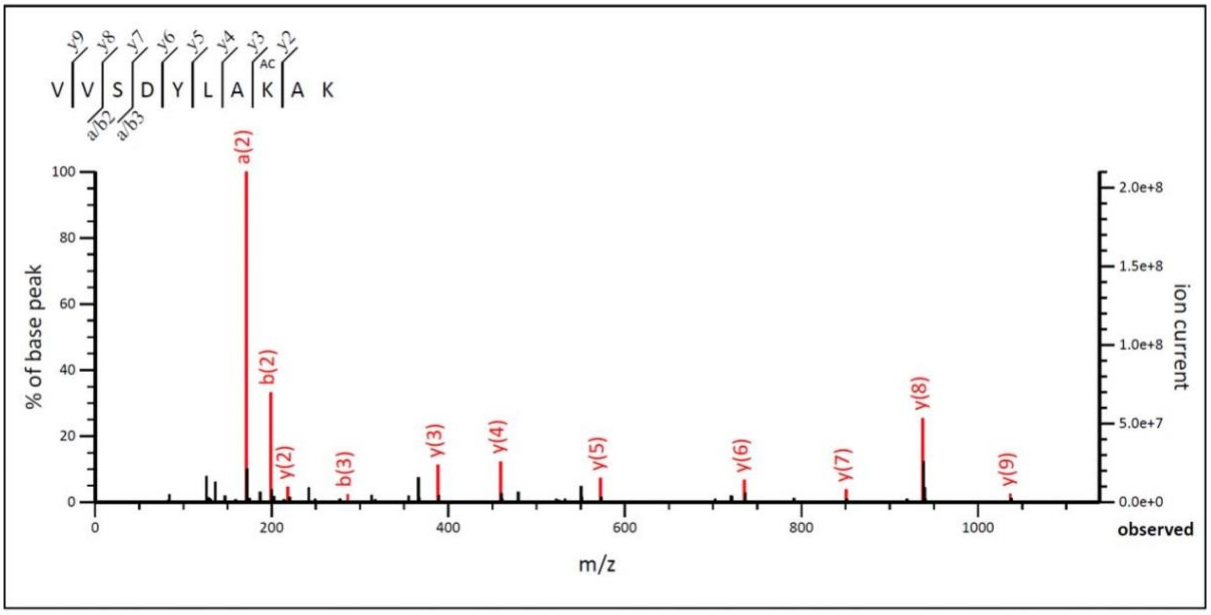

#	a	a^{++}	a*	a*$^{++}$	b	b^{++}	b*	b*$^{++}$	Seq.	y	y^{++}	y*	y*$^{++}$	#
1	72.0808	36.5440			100.0757	50.5415			V					10
2	171.1492	86.0782			199.1441	100.0757			V	*1036.5673*	518.7873	1019.5408	510.2740	9
3	258.1812	129.5942			286.1761	143.5917			S	*937.4989*	469.2531	920.4724	460.7398	8
4	373.2082	187.1077			401.2031	201.1052			D	*850.4669*	425.7371	833.4403	417.2238	7
5	536.2715	268.6394			564.2664	282.6368			Y	*735.4400*	368.2236	718.4134	359.7103	6
6	649.3556	325.1814			677.3505	339.1789			L	*572.3766*	286.6920	555.3501	278.1787	5
7	720.3927	360.7000			748.3876	374.6974			A	*459.2926*	230.1499	442.2660	221.6366	4
8	890.4982	445.7527	873.4716	437.2395	918.4931	459.7502	901.4666	451.2369	K	*388.2554*	194.6314	371.2289	186.1181	3
9	961.5353	481.2713	944.5088	472.7580	989.5302	495.2688	972.5037	486.7555	A	*218.1499*	109.5786	201.1234	101.0653	2
10									K	147.1128	74.0600	130.0863	65.5468	1

Figure S4. LC-MS/MS analysis of AcnA 482-AcK. The tandem mass spectrum of the peptide (residues 475-484) VVSDYLAKAK from purified AcnA 482-AcK. KAC denotes AcK incorporation. The partial sequence of the peptide containing the AcK can be read from the annotated a/b or y ion series. Matched peaks are in red.

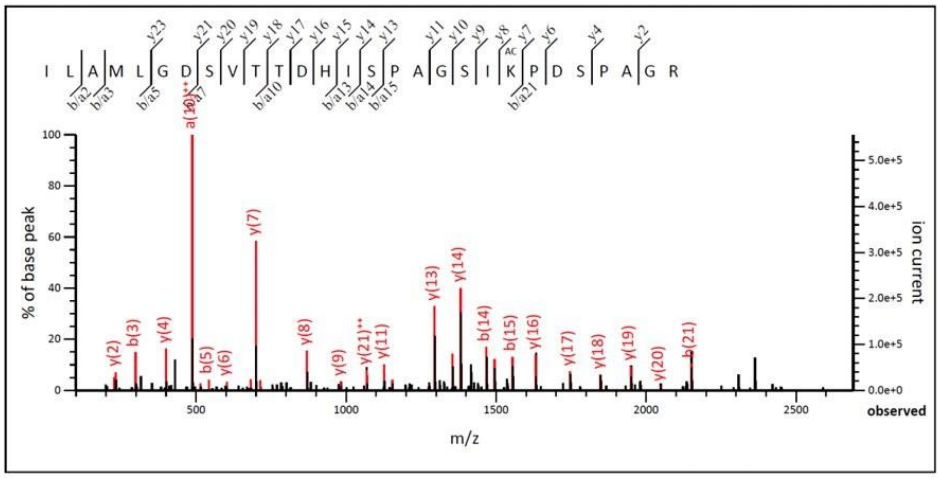

#	a	a^{++}	a*	a*$^{++}$	b	b^{++}	b*	b*$^{++}$	Seq.	y	y^{++}	y*	y*$^{++}$	#
1	86.0964	43.5519			114.0913	57.5493			I					28
2	199.1805	100.0939			**227.1754**	114.0913			L	2735.3669	1368.1871	2718.3403	1359.6738	27
3	270.2176	135.6124			**298.2125**	149.6099			A	2622.2828	1311.6450	2605.2563	1303.1318	26
4	401.2581	201.1327			429.2530	215.1301			M	2551.2457	1276.1265	2534.2191	1267.6132	25
5	**514.3422**	257.6747			**542.3371**	271.6722			L	2420.2052	1210.6062	2403.1787	1202.0930	24
6	571.3636	286.1854			599.3585	300.1829			G	2307.1211	**1154.0642**	2290.0946	1145.5509	23
7	686.3906	343.6989			**714.3855**	357.6964			D	2250.0997	1125.5535	2233.0731	1117.0402	22
8	773.4226	387.2149			801.4175	401.2124			S	2135.0727	**1068.0400**	2118.0462	1059.5267	21
9	872.4910	436.7491			900.4859	450.7466			V	***2048.0407***	1024.5240	2031.0142	1016.0107	20
10	973.5387	**487.2730**			1001.5336	501.2704			T	***1948.9723***	974.9898	1931.9457	966.4765	19
11	1074.5864	537.7968			1102.5813	551.7943			T	***1847.9246***	924.4659	1830.8981	915.9527	18
12	1189.6133	595.3103			1217.6082	609.3077			D	***1746.8769***	873.9421	1729.8504	865.4288	17
13	1326.6722	663.8397			**1354.6671**	677.8372			H	***1631.8500***	816.4286	1614.8234	807.9154	16
14	1439.7563	720.3818			**1467.7512**	734.3792			I	***1494.7911***	747.8992	1477.7645	739.3859	15
15	1526.7883	763.8978			**1554.7832**	777.8952			S	***1381.7070***	691.3571	1364.6805	682.8439	14
16	1623.8411	812.4242			1651.8360	826.4216			P	***1294.6750***	647.8411	1277.6484	639.3279	13
17	1694.8782	847.9427			1722.8731	861.9402			A	1197.6222	599.3148	1180.5957	590.8015	12
18	1751.8996	876.4535			1779.8946	890.4509			G	***1126.5851***	563.7962	1109.5586	555.2829	11
19	1838.9317	919.9695			1866.9266	933.9669			S	***1069.5636***	535.2855	1052.5371	526.7722	10
20	1952.0157	976.5115			1980.0107	990.5090			I	***982.5316***	491.7694	965.5051	483.2562	9
21	2122.1213	1061.5643	2105.0947	1053.0510	**2150.1162**	1075.5617	2133.0896	1067.0485	K	***869.4476***	435.2274	852.4210	426.7141	8
22	2219.1740	1110.0907	2202.1475	1101.5774	2247.1689	1124.0881	2230.1424	1115.5748	P	***699.3420***	350.1747	682.3155	341.6614	7
23	2334.2010	1167.6041	2317.1744	1159.0909	2362.1959	1181.6016	2345.1693	1173.0883	D	***602.2893***	301.6483	585.2627	293.1350	6
24	2421.2330	1211.1201	2404.2065	1202.6069	2449.2279	1225.1176	2432.2014	1216.6043	S	***487.2623***	244.1348	470.2358	235.6215	5
25	2518.2858	1259.6465	2501.2592	1251.1332	2546.2807	1273.6440	2529.2541	1265.1307	P	***400.2303***	200.6188	383.2037	192.1055	4
26	2589.3229	1295.1651	2572.2963	1286.6518	2617.3178	1309.1625	2600.2912	1300.6493	A	303.1775	152.0924	286.1510	143.5791	3
27	2646.3443	1323.6758	2629.3178	1315.1625	2674.3393	1337.6733	2657.3127	1329.1600	G	***232.1404***	116.5738	215.1139	108.0606	2
28									R	175.1190	88.0631	158.0924	79.5498	1

Figure S5. LC-MS/MS analysis of AcnA 684-AcK. The tandem mass spectrum of the peptide (residues 664-691) ILAMLGDSVTTDHISPAGSIKPDSPAGR from purified AcnA 684-AcK. KAC denotes AcK incorporation. The partial sequence of the peptide containing the AcK can be

read from the annotated a/b or y ion series. Matched peaks are in red.

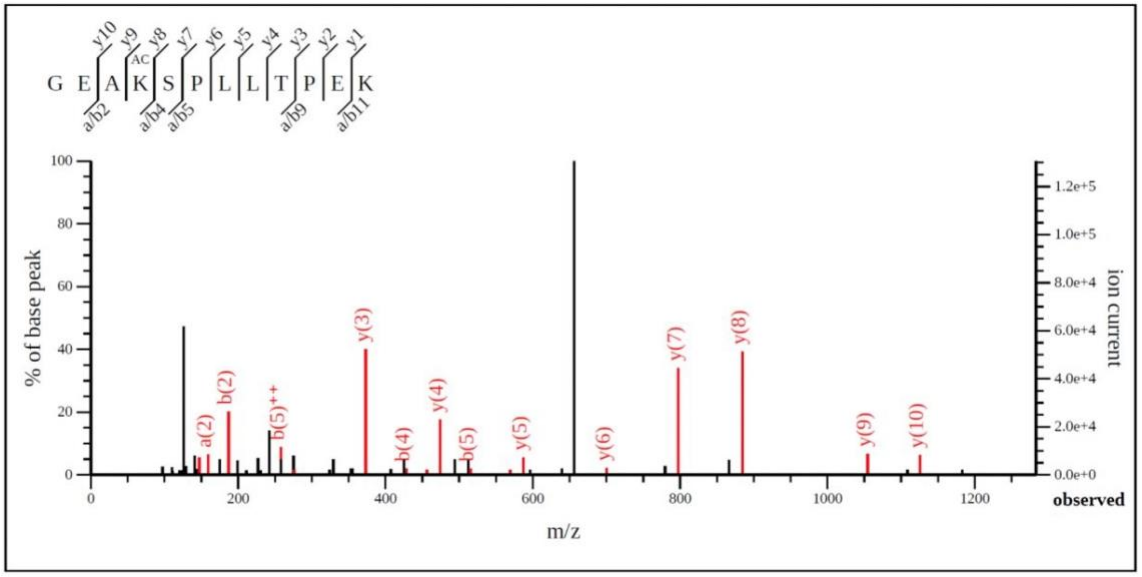

#	a	a^{++}	a*	a^{*+++}	b	b^{++}	b*	b^{*+++}	Seq.	y	y^{++}	y*	y^{*+++}	#
1	30.0338	15.5206			58.0287	29.5180			G					12
2	**159.0764**	80.0418			**187.0713**	94.0393			E	1254.6940	627.8506	1237.6674	619.3374	11
3	230.1135	115.5604			**258.1084**	129.5579			A	*1125.6514*	563.3293	1108.6249	554.8161	10
4	400.2191	200.6132	383.1925	192.0999	**428.2140**	214.6106	411.1874	206.0974	K	*1054.6143*	527.8108	1037.5877	519.2975	9
5	487.2511	244.1292	470.2245	235.6159	**515.2460**	**258.1266**	498.2195	249.6134	S	*884.5088*	442.7580	867.4822	434.2447	8
6	584.3039	292.6556	567.2773	284.1423	612.2988	306.6530	595.2722	298.1397	P	*797.4767*	399.2420	780.4502	390.7287	7
7	697.3879	349.1976	680.3614	340.6843	725.3828	363.1951	708.3563	354.6818	L	*700.4240*	350.7156	683.3974	342.2023	6
8	810.4720	405.7396	793.4454	397.2264	838.4669	419.7371	821.4403	411.2238	L	*587.3399*	294.1736	570.3134	285.6603	5
9	911.5197	**456.2635**	894.4931	447.7502	939.5146	470.2609	922.4880	461.7477	T	*474.2558*	237.6316	457.2293	229.1183	4
10	1008.5724	504.7898	991.5459	496.2766	1036.5673	518.7873	1019.5408	510.2740	P	*373.2082*	187.1077	356.1816	178.5944	3
11	1137.6150	**569.3111**	1120.5885	560.7979	1165.6099	583.3086	1148.5834	574.7953	E	*276.1554*	138.5813	259.1288	130.0681	2
12									K	*147.1128*	74.0600	130.0863	65.5468	1

Figure S6. LC-MS/MS analysis of AcnB 77-AcK. The tandem mass spectrum of the peptide (residues 74-85) GEAKSPLLTPEK from purified AcnB 77-AcK. KAC denotes AcK incorporation. The partial sequence of the peptide containing the AcK can be read from the annotated a/b or y ion series. Matched peaks are in red.

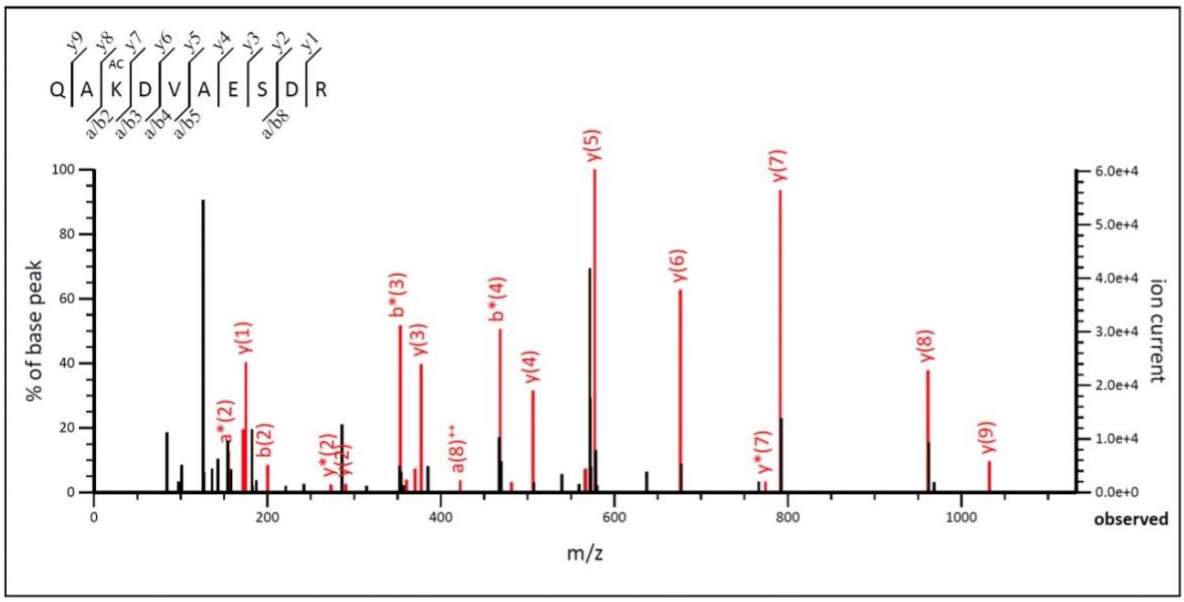

#	a	a^{++}	a*	a*$^{++}$	b	b^{++}	b*	b*$^{++}$	Seq.	y	y^{++}	y*	y*$^{++}$	#
1	101.0709	51.0391	84.0444	42.5258	129.0659	65.0366	112.0393	56.5233	Q					10
2	**172.1081**	86.5577	155.0815	78.0444	**200.1030**	100.5551	183.0764	92.0418	A	***1032.4956***	516.7515	1015.4691	508.2382	9
3	342.2136	171.6104	325.1870	163.0972	**370.2085**	185.6079	353.1819	177.0946	K	***961.4585***	**481.2329**	944.4320	472.7196	8
4	457.2405	229.1239	440.2140	220.6106	485.2354	243.1214	468.2089	234.6081	D	***791.3530***	396.1801	774.3264	387.6669	7
5	556.3089	278.6581	539.2824	270.1448	584.3039	292.6556	567.2773	284.1423	V	***676.3260***	338.6667	659.2995	330.1534	6
6	627.3461	314.1767	610.3195	305.6634	655.3410	328.1741	638.3144	319.6608	A	***577.2576***	289.1325	560.2311	280.6192	5
7	756.3886	378.6980	739.3621	370.1847	784.3836	392.6954	767.3570	384.1821	E	***506.2205***	253.6139	489.1940	245.1006	4
8	843.4207	**422.2140**	826.3941	413.7007	871.4156	436.2114	854.3890	427.6982	S	***377.1779***	189.0926	360.1514	180.5793	3
9	958.4476	479.7274	941.4211	471.2142	986.4425	493.7249	969.4160	485.2116	D	***290.1459***	145.5766	273.1193	137.0633	2
10									R	***175.1190***	88.0631	158.0924	79.5498	1

Figure S7. LC-MS/MS analysis of AcnB 373-AcK. The tandem mass spectrum of the peptide (residues 371-380) QAKDVAESDR from purified AcnB 373-AcK. KAC denotes AcK incorporation. The partial sequence of the peptide containing the AcK can be read from the annotated a/b or y ion series. Matched peaks are in red.

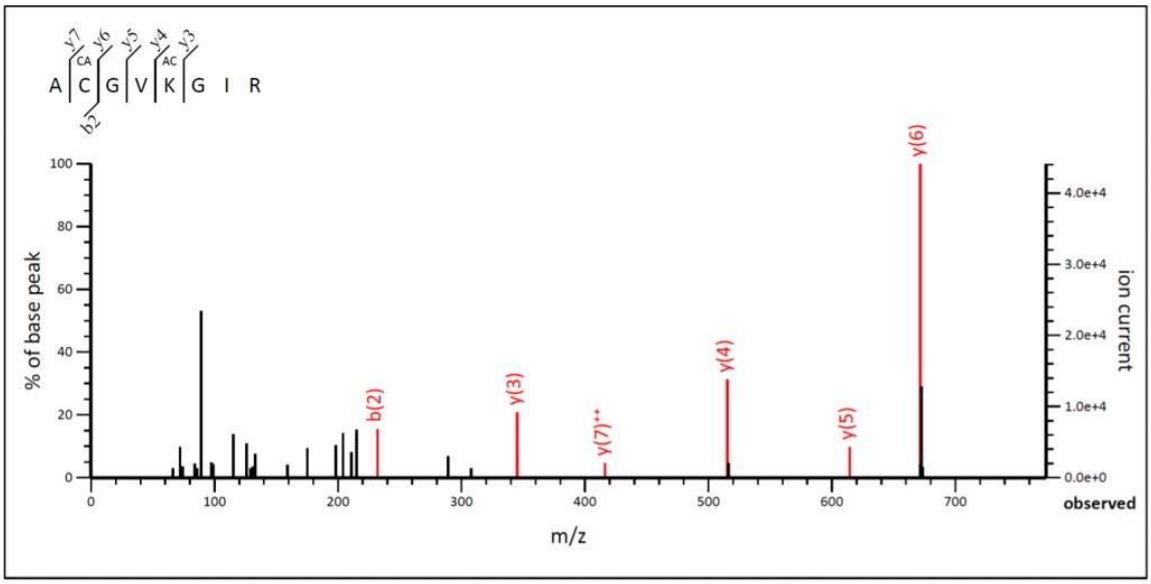

#	a	a^{++}	a*	a*$^{++}$	b	b^{++}	b*	b*$^{++}$	Seq.	y	y^{++}	y*	y*$^{++}$	#
1	44.0495	22.5284			72.0444	36.5258			A					8
2	204.0801	102.5437			**232.0750**	116.5412			C	831.4505	**416.2289**	814.4240	407.7156	7
3	261.1016	131.0544			289.0965	145.0519			G	***671.4199***	336.2136	654.3933	327.7003	6
4	360.1700	180.5886			388.1649	194.5861			V	***614.3984***	307.7028	597.3719	299.1896	5
5	530.2755	265.6414	513.2490	257.1281	558.2704	279.6389	541.2439	271.1256	K	***515.3300***	258.1686	498.3035	249.6554	4
6	587.2970	294.1521	570.2704	285.6389	615.2919	308.1496	598.2654	299.6363	G	***345.2245***	173.1159	328.1979	164.6026	3
7	700.3811	350.6942	683.3545	342.1809	728.3760	364.6916	711.3494	356.1784	I	288.2030	144.6051	271.1765	136.0919	2
8									R	175.1190	88.0631	158.0924	79.5498	1

Figure S8. LC-MS/MS analysis of AcnB 396-AcK. The tandem mass spectrum of the peptide (residues 392-399) ACGVKGIR from purified AcnB 396-AcK. KAC denotes AcK incorporation. The partial sequence of the peptide containing the AcK can be read from the annotated a/b or y ion series. Matched peaks are in red.

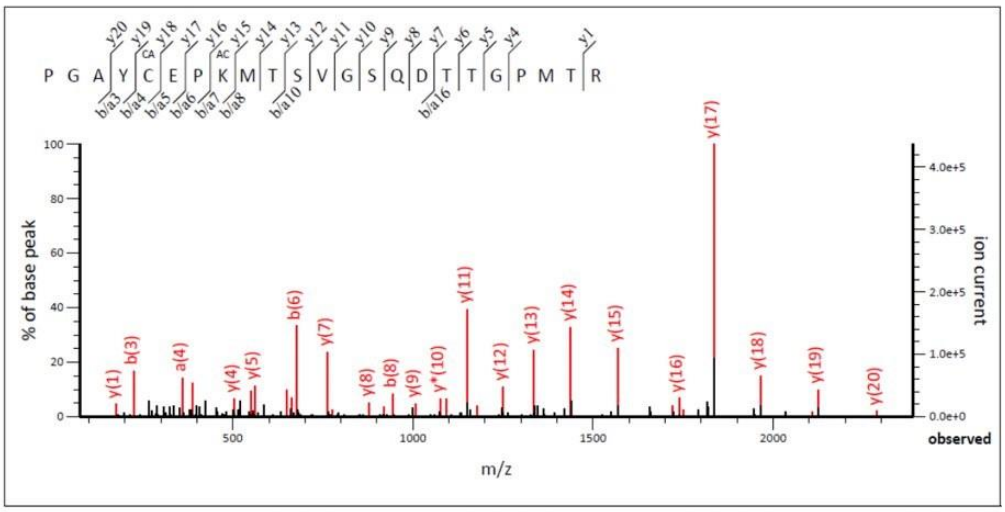

#	a	a^{++}	a*	a*$^{++}$	b	b^{++}	b*	b*$^{++}$	Seq.	y	y^{++}	y*	y*$^{++}$	#
1	70.0651	35.5362			98.0600	49.5337			P					23
2	127.0866	64.0469			155.0815	78.0444			G	2416.0578	1208.5325	2399.0312	1200.0192	22
3	198.1237	99.5655			**226.1186**	113.5629			A	2359.0363	1180.0218	2342.0097	1171.5085	21
4	**361.1870**	181.0972			**389.1819**	195.0946			Y	*2287.9992*	1144.5032	2270.9726	1135.9900	20
5	521.2177	261.1125			**549.2126**	275.1099			C	*2124.9359*	1062.9716	2107.9093	1054.4583	19
6	**650.2603**	325.6338			**678.2552**	339.6312			E	*1964.9052*	982.9562	1947.8787	974.4430	18
7	747.3130	374.1602			**775.3080**	388.1576			P	*1835.8626*	**918.4349**	1818.8361	909.9217	17
8	917.4186	459.2129	900.3920	450.6996	**945.4135**	473.2104	928.3869	464.6971	K	*1738.8098*	869.9086	1721.7833	861.3953	16
9	1048.4591	524.7332	1031.4325	516.2199	**1076.4540**	538.7306	1059.4274	530.2173	M	*1568.7043*	784.8558	1551.6778	776.3425	15
10	1149.5067	575.2570	1132.4802	566.7437	**1177.5016**	589.2545	1160.4751	580.7412	T	*1437.6638*	719.3356	1420.6373	710.8223	14
11	1236.5388	618.7730	1219.5122	610.2597	1264.5337	632.7705	1247.5071	624.2572	S	*1336.6162*	668.8117	1319.5896	660.2984	13
12	1335.6072	668.3072	1318.5806	659.7939	1363.6021	682.3047	1346.5755	673.7914	V	*1249.5841*	625.2957	1232.5576	616.7824	12
13	1392.6286	696.8180	1375.6021	688.3047	1420.6236	710.8154	1403.5970	702.3021	G	*1150.5157*	575.7615	1133.4892	567.2482	11
14	1479.6607	740.3340	1462.6341	731.8207	1507.6556	754.3314	1490.6290	745.8182	S	*1093.4943*	547.2508	1076.4677	538.7375	10
15	1607.7192	804.3633	1590.6927	795.8500	1635.7142	818.3607	1618.6876	809.8474	Q	*1006.4622*	503.7347	989.4357	495.2215	9
16	1722.7462	861.8767	1705.7196	853.3635	**1750.7411**	875.8742	1733.7146	867.3609	D	*878.4036*	439.7055	861.3771	431.1922	8
17	1823.7939	912.4006	1806.7673	903.8873	1851.7888	926.3980	1834.7622	917.8848	T	*763.3767*	382.1920	746.3502	373.6787	7
18	1924.8415	962.9244	1907.8150	954.4111	1952.8365	976.9219	1935.8099	968.4086	T	*662.3290*	331.6681	645.3025	323.1549	6
19	1981.8630	991.4351	1964.8365	982.9219	2009.8579	1005.4326	1992.8314	996.9193	G	*561.2813*	281.1443	544.2548	272.6310	5
20	2078.9158	1039.9615	2061.8892	1031.4482	2106.9107	1053.9590	2089.8841	1045.4457	P	*504.2599*	252.6336	487.2333	244.1203	4
21	2209.9563	1105.4818	2192.9297	1096.9685	2237.9512	1119.4792	2220.9246	1110.9659	M	407.2071	204.1072	390.1806	195.5939	3
22	2311.0039	1156.0056	2293.9774	1147.4923	2338.9988	1170.0031	2321.9723	1161.4898	T	276.1666	138.5870	259.1401	130.0737	2
23									R	*175.1190*	88.0631	158.0924	79.5498	1

Figure S9. LC-MS/MS analysis of AcnB 407-AcK. The tandem mass spectrum of the peptide (residues 400-422) PGAYCEPKMTSVGSQDTTGPMTR from purified AcnB 407-AcK. KAC denotes AcK incorporation. The partial sequence of the peptide containing the AcK can be read from the annotated a/b or y ion series. Matched peaks are in red.

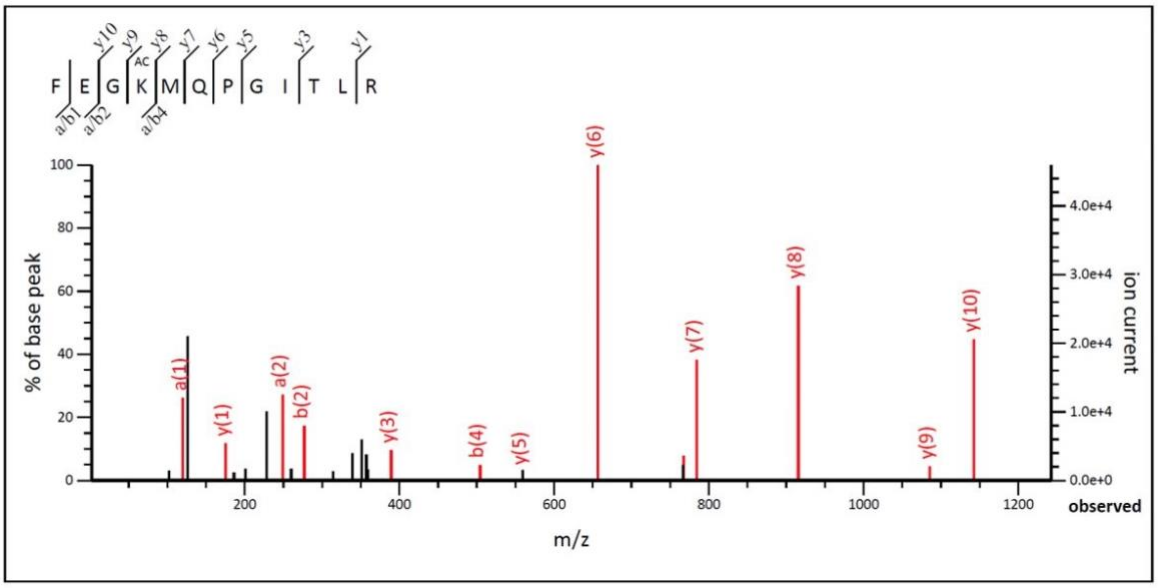

#	a	a^{++}	a*	a^{*++}	b	b^{++}	b*	b^{*++}	Seq.	y	y^{++}	y*	y^{*++}	#
1	**120.0808**	60.5440			148.0757	74.5415			F					12
2	**249.1234**	125.0653			**277.1183**	139.0628			E	1271.6776	636.3425	1254.6511	627.8292	11
3	306.1448	153.5761			334.1397	167.5735			G	***1142.6350***	571.8212	1125.6085	563.3079	10
4	476.2504	238.6288	459.2238	230.1155	**504.2453**	252.6263	487.2187	244.1130	K	***1085.6136***	543.3104	1068.5870	534.7972	9
5	607.2908	304.1491	590.2643	295.6358	635.2858	318.1465	618.2592	309.6332	M	***915.5080***	458.2577	898.4815	449.7444	8
6	735.3494	368.1783	718.3229	359.6651	763.3443	382.1758	746.3178	373.6625	Q	***784.4676***	392.7374	**767.4410**	384.2241	7
7	832.4022	416.7047	815.3756	408.1915	860.3971	430.7022	843.3706	422.1889	P	***656.4090***	328.7081	639.3824	320.1949	6
8	889.4237	445.2155	872.3971	436.7022	917.4186	459.2129	900.3920	450.6996	G	***559.3562***	280.1817	542.3297	271.6685	5
9	1002.5077	501.7575	985.4812	493.2442	1030.5026	515.7550	1013.4761	507.2417	I	502.3348	251.6710	485.3082	243.1577	4
10	1103.5554	552.2813	1086.5288	543.7681	1131.5503	566.2788	1114.5238	557.7655	T	***389.2507***	195.1290	372.2241	186.6157	3
11	1216.6395	608.8234	1199.6129	600.3101	1244.6344	622.8208	1227.6078	614.3075	L	288.2030	144.6051	271.1765	136.0919	2
12									R	***175.1190***	88.0631	158.0924	79.5498	1

Figure S10. LC-MS/MS analysis of AcnB 539-AcK. The tandem mass spectrum of the peptide (residues 536-547) FEGKMQPGITLR from purified AcnB 539-AcK. KAC denotes AcK incorporation. The partial sequence of the peptide containing the AcK can be read from the annotated a/b or y ion series. Matched peaks are in red.

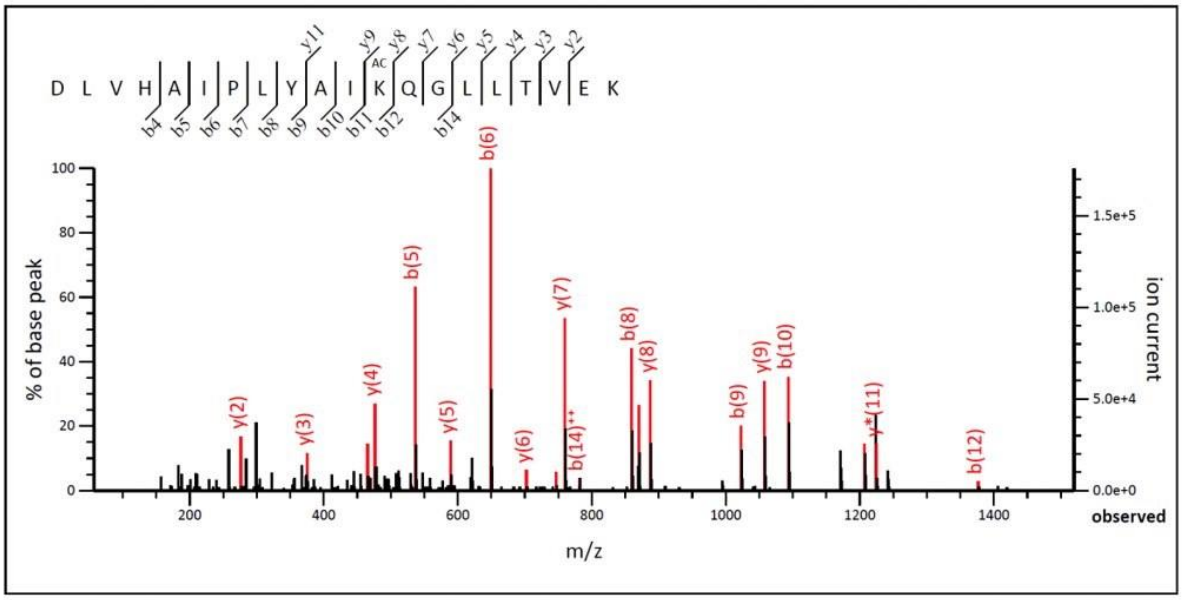

#	a	a^{++}	a*	a*$^{++}$	b	b^{++}	b*	b*$^{++}$	Seq.	y	y^{++}	y*	y*$^{++}$	#
1	88.0393	44.5233			116.0342	58.5207			D					20
2	201.1234	101.0653			229.1183	115.0628			L	2148.2791	1074.6432	2131.2525	1066.1299	19
3	300.1918	150.5995			328.1867	164.5970			V	2035.1950	1018.1012	2018.1685	1009.5879	18
4	437.2507	219.1290			***465.2456***	233.1264			H	1936.1266	968.5669	1919.1001	960.0537	17
5	508.2878	254.6475			***536.2827***	268.6450			A	1799.0677	900.0375	1782.0412	891.5242	16
6	621.3719	311.1896			***649.3668***	325.1870			I	1728.0306	864.5189	1711.0040	856.0057	15
7	718.4246	359.7160			***746.4196***	373.7134			P	1614.9465	807.9769	1597.9200	799.4636	14
8	831.5087	416.2580			***859.5036***	430.2554			L	1517.8938	**759.4505**	1500.8672	750.9372	13
9	994.5720	497.7897			***1022.5669***	511.7871			Y	1404.8097	702.9085	1387.7831	694.3952	12
10	1065.6091	533.3082			***1093.6041***	547.3057			A	1241.7464	621.3768	1224.7198	612.8635	11
11	1178.6932	589.8502			***1206.6881***	603.8477			I	1170.7093	585.8583	1153.6827	577.3450	10
12	1348.7987	674.9030	1331.7722	666.3897	***1376.7937***	688.9005	1359.7671	680.3872	K	***1057.6252***	529.3162	1040.5986	520.8030	9
13	1476.8573	738.9323	1459.8308	730.4190	1504.8522	752.9298	1487.8257	744.4165	Q	***887.5197***	444.2635	**870.4931**	435.7502	8
14	1533.8788	767.4430	1516.8522	758.9298	1561.8737	**781.4405**	1544.8471	772.9272	G	***759.4611***	380.2342	742.4345	371.7209	7
15	1646.9628	823.9851	1629.9363	815.4718	1674.9578	837.9825	1657.9312	829.4692	L	***702.4396***	351.7234	685.4131	343.2102	6
16	1760.0469	880.5271	1743.0204	872.0138	1788.0418	894.5245	1771.0153	886.0113	L	***589.3556***	295.1814	572.3290	286.6681	5
17	1861.0946	931.0509	1844.0680	922.5377	1889.0895	945.0484	1872.0629	936.5351	T	***476.2715***	238.6394	459.2449	230.1261	4
18	1960.1630	980.5851	1943.1364	972.0719	1988.1579	994.5826	1971.1314	986.0693	V	***375.2238***	188.1155	358.1973	179.6023	3
19	2089.2056	1045.1064	2072.1790	1036.5932	2117.2005	1059.1039	2100.1740	1050.5906	E	***276.1554***	138.5813	259.1288	130.0681	2
20									K	147.1128	74.0600	130.0863	65.5468	1

Figure S11. LC-MS/MS analysis of AcnB 559-AcK. The tandem mass spectrum of the peptide (residues 548-567) DLVHAIPLYAIKQGLLTVEK from purified AcnB 559-AcK. KAC denotes AcK incorporation. The partial sequence of the peptide containing the AcK can be read from the annotated a/b or y ion series. Matched peaks are in red.

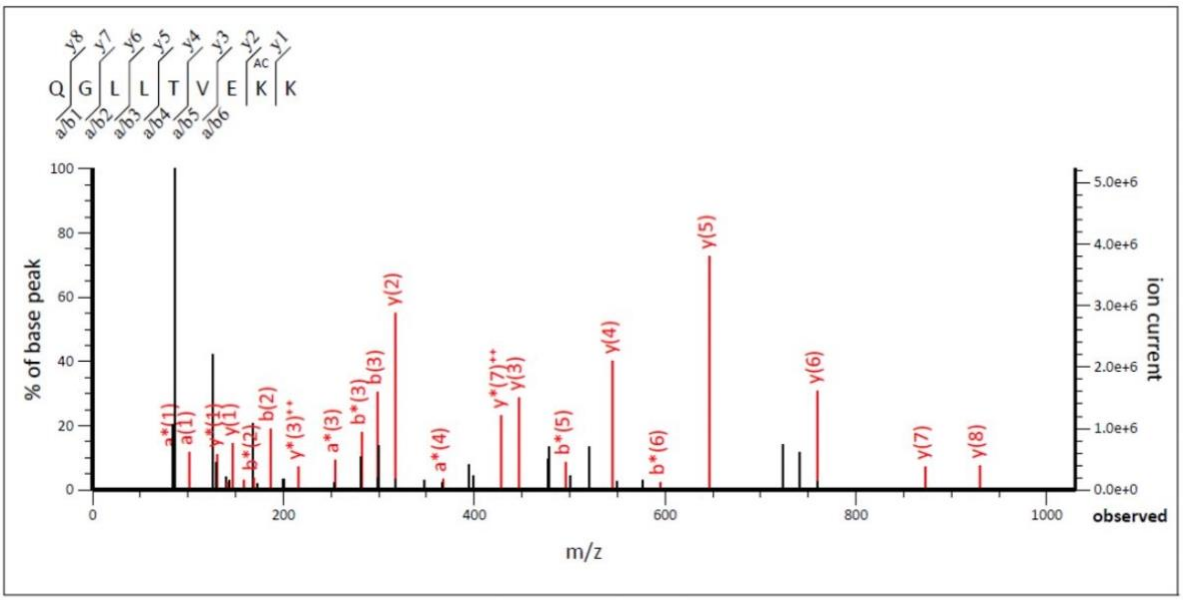

#	a	a^{++}	a*	a*$^{++}$	b	b^{++}	b*	b*$^{++}$	Seq.	y	y^{++}	y*	y*$^{++}$
1	**101.0709**	51.0391	**84.0444**	42.5258	**129.0659**	65.0366	112.0393	56.5233	Q				
2	**158.0924**	79.5498	**141.0659**	71.0366	**186.0873**	93.5473	**169.0608**	85.0340	G	**929.5666**	465.2869	912.5401	456.7737
3	271.1765	136.0919	**254.1499**	127.5786	**299.1714**	150.0893	**282.1448**	141.5761	L	**872.5451**	436.7762	855.5186	**428.2629**
4	384.2605	192.6339	**367.2340**	184.1206	412.2554	206.6314	395.2289	198.1181	L	**759.4611**	380.2342	742.4345	371.7209
5	485.3082	243.1577	468.2817	234.6445	513.3031	257.1552	**496.2766**	248.6419	T	**646.3770**	323.6921	629.3505	315.1789
6	584.3766	292.6920	567.3501	284.1787	612.3715	306.6894	**595.3450**	298.1761	V	**545.3293**	273.1683	528.3028	264.6550
7	713.4192	357.2132	696.3927	348.7000	741.4141	371.2107	724.3876	362.6974	E	**446.2609**	223.6341	429.2344	**215.1208**
8	883.5247	442.2660	866.4982	433.7527	911.5197	456.2635	894.4931	447.7502	K	**317.2183**	159.1128	300.1918	150.5995
9									K	**147.1128**	74.0600	**130.0863**	65.5468

Figure S12. LC-MS/MS analysis of AcnB 567-AcK. The tandem mass spectrum of the peptide (residues 560-568) QGLLTVEKK from purified AcnB 567-AcK. KAC denotes AcK incorporation. The partial sequence of the peptide containing the AcK can be read from the annotated a/b or y ion series. Matched peaks are in red.

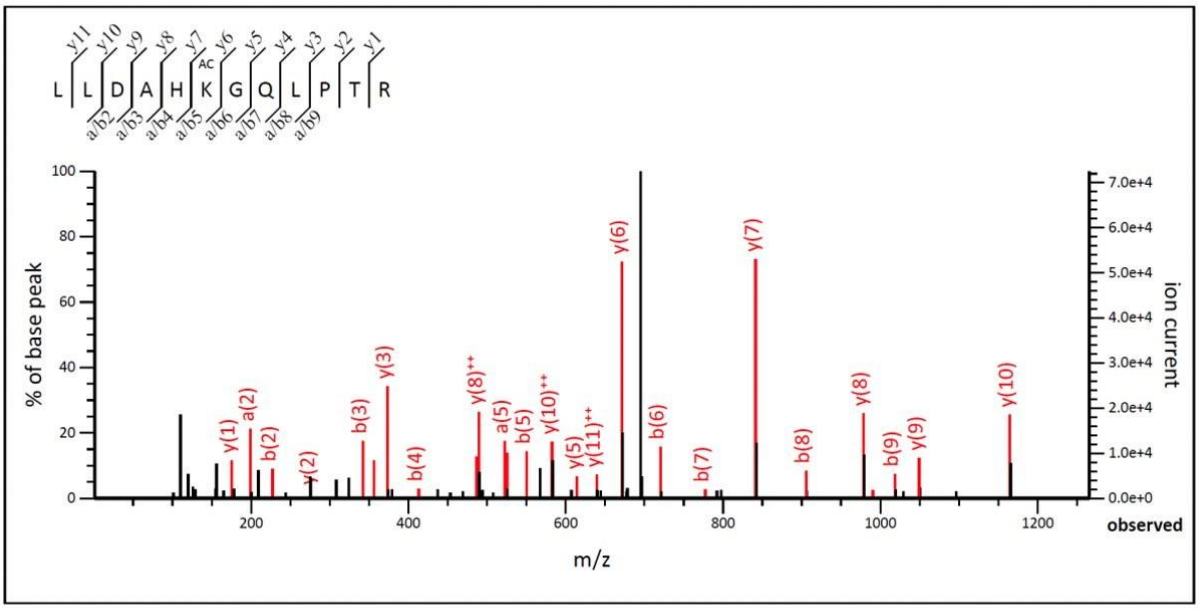

#	a	a^{++}	a*	a*$^{++}$	b	b^{++}	b*	b*$^{++}$	Seq.	y	y^{++}	y*	y*$^{++}$	#
1	86.0964	43.5519			114.0913	57.5493			L					12
2	**199.1805**	100.0939			**227.1754**	114.0913			L	1277.6961	**639.3517**	1260.6695	630.8384	11
3	314.2074	157.6074			**342.2023**	171.6048			D	***1164.6120***	**582.8096**	1147.5854	574.2964	10
4	385.2445	193.1259			**413.2395**	207.1234			A	***1049.5851***	**525.2962**	1032.5585	516.7829	9
5	**522.3035**	261.6554			**550.2984**	275.6528			H	***978.5479***	**489.7776**	961.5214	481.2643	8
6	692.4090	346.7081	675.3824	338.1949	**720.4039**	360.7056	703.3774	352.1923	K	***841.4890***	421.2482	824.4625	412.7349	7
7	749.4305	375.2189	732.4039	366.7056	**777.4254**	389.2163	760.3988	380.7030	G	***671.3835***	336.1954	654.3570	327.6821	6
8	877.4890	439.2482	860.4625	430.7349	**905.4839**	453.2456	888.4574	444.7323	Q	***614.3620***	307.6847	597.3355	299.1714	5
9	**990.5731**	495.7902	973.5465	487.2769	**1018.5680**	509.7876	1001.5415	501.2744	L	***486.3035***	243.6554	469.2769	235.1421	4
10	1087.6259	544.3166	1070.5993	535.8033	1115.6208	558.3140	1098.5942	549.8007	P	***373.2194***	187.1133	**356.1928**	178.6001	3
11	1188.6735	594.8404	1171.6470	586.3271	1216.6685	608.8379	1199.6419	600.3246	T	***276.1666***	138.5870	259.1401	130.0737	2
12									R	***175.1190***	88.0631	158.0924	79.5498	1

Figure S13. LC-MS/MS analysis of AcnB 728-AcK. The tandem mass spectrum of the peptide (residues 723-734) LLDAHKGQLPTR from purified AcnB 728-AcK. KAC denotes AcK incorporation. The partial sequence of the peptide containing the AcK can be read from the annotated a/b or y ion series. Matched peaks are in red.

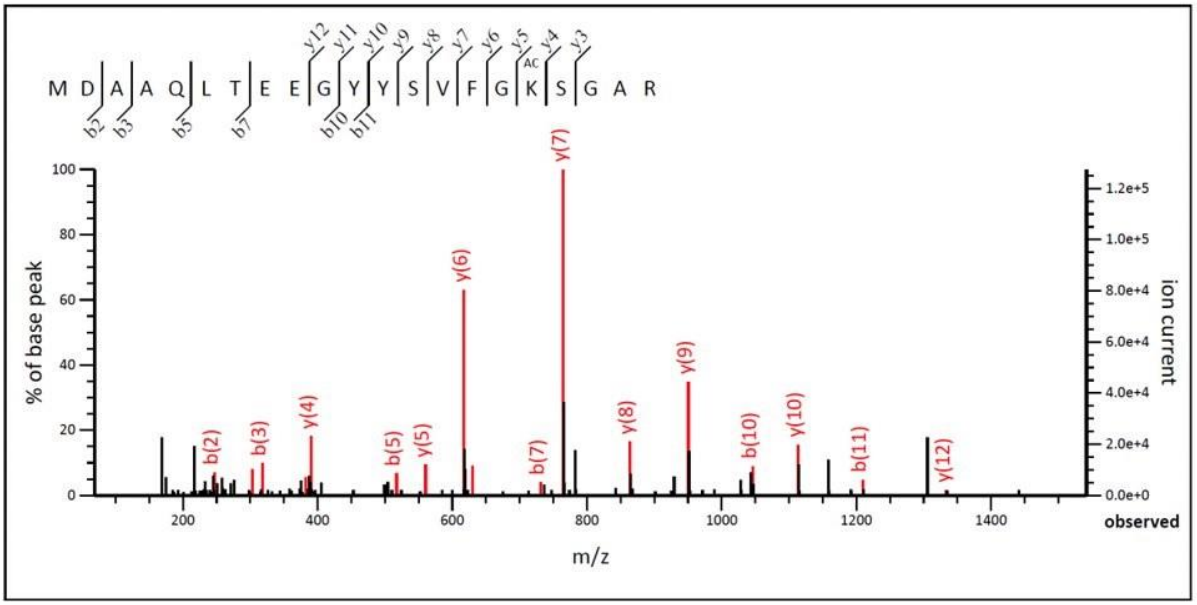

#	a	a^{++}	a*	a*$^{++}$	b	b^{++}	b*	b*$^{++}$	Seq.	y	y^{++}	y*	y*$^{++}$	#
1	104.0528	52.5301			132.0478	66.5275			M					21
2	219.0798	110.0435			***247.0747***	124.0410			D	2191.0302	1096.0187	2174.0037	1087.5055	20
3	290.1169	145.5621			***318.1118***	159.5595			A	2076.0033	1038.5053	2058.9767	1029.9920	19
4	361.1540	181.0806			389.1489	195.0781			A	2004.9661	1002.9867	1987.9396	994.4734	18
5	489.2126	245.1099	472.1860	236.5967	***517.2075***	259.1074	500.1810	250.5941	Q	1933.9290	967.4682	1916.9025	958.9549	17
6	602.2967	301.6520	585.2701	293.1387	***630.2916***	315.6494	613.2650	307.1362	L	1805.8705	903.4389	1788.8439	894.9256	16
7	703.3443	352.1758	686.3178	343.6625	***731.3393***	366.1733	714.3127	357.6600	T	1692.7864	846.8968	1675.7598	838.3836	15
8	832.3869	416.6971	815.3604	408.1838	860.3818	430.6946	843.3553	422.1813	E	1591.7387	796.3730	1574.7122	787.8597	14
9	961.4295	481.2184	944.4030	472.7051	989.4244	495.2159	972.3979	486.7026	E	1462.6961	731.8517	1445.6696	723.3384	13
10	1018.4510	509.7291	1001.4244	501.2159	***1046.4459***	523.7266	1029.4194	515.2133	G	***1333.6535***	667.3304	1316.6270	658.8171	12
11	1181.5143	591.2608	1164.4878	582.7475	***1209.5092***	605.2583	1192.4827	596.7450	Y	1276.6321	638.8197	1259.6055	630.3064	11
12	1344.5776	672.7925	1327.5511	664.2792	1372.5726	686.7899	1355.5460	678.2766	Y	***1113.5687***	557.2880	1096.5422	548.7747	10
13	1431.6097	716.3085	1414.5831	707.7952	1459.6046	730.3059	1442.5780	721.7927	S	***950.5054***	475.7563	933.4789	467.2431	9
14	1530.6781	765.8427	1513.6515	757.3294	1558.6730	779.8401	1541.6465	771.3269	V	***863.4734***	432.2403	846.4468	423.7271	8
15	1677.7465	839.3769	1660.7200	830.8636	1705.7414	853.3743	1688.7149	844.8611	F	***764.4050***	***382.7061***	747.3784	374.1928	7
16	1734.7680	867.8876	1717.7414	859.3743	1762.7629	881.8851	1745.7363	873.3718	G	***617.3366***	309.1719	600.3100	300.6586	6
17	1904.8735	952.9404	1887.8469	944.4271	1932.8684	966.9378	1915.8419	958.4246	K	***560.3151***	280.6612	543.2885	272.1479	5
18	1991.9055	996.4564	1974.8790	987.9431	2019.9004	1010.4539	2002.8739	1001.9406	S	***390.2096***	195.6084	373.1830	187.0951	4
19	2048.9270	1024.9671	2031.9004	1016.4539	2076.9219	1038.9646	2059.8954	1030.4513	G	***303.1775***	152.0924	286.1510	143.5791	3
20	2119.9641	1060.4857	2102.9376	1051.9724	2147.9590	1074.4831	2130.9325	1065.9699	A	246.1561	123.5817	229.1295	115.0684	2
21									R	175.1190	88.0631	158.0924	79.5498	1

Figure S14. LC-MS/MS analysis of AcnB 759-AcK. The tandem mass spectrum of the peptide (residues 743-763) MDAAQLTEEGYYSVFGKSGAR from purified AcnB 759-AcK. KAC denotes AcK incorporation. The partial sequence of the peptide containing the AcK can be read from the annotated a/b or y ion series. Matched peaks are in red.

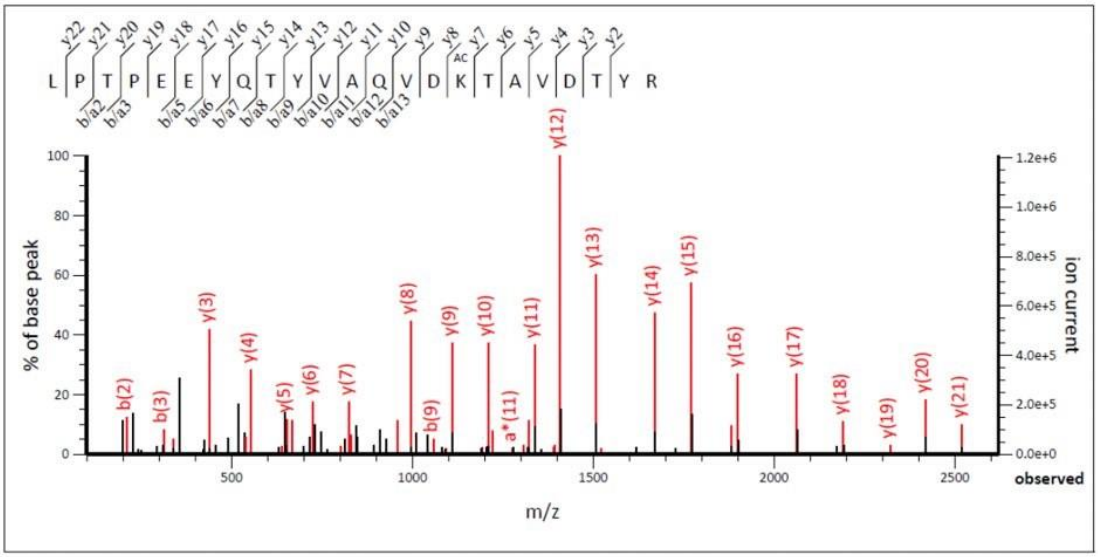

#	a	a^{++}	a*	a*$^{++}$	b	b^{++}	b*	b*$^{++}$	Seq.	y	y^{++}	y*	y*$^{++}$	#
1	86.0964	43.5519			114.0913	57.5493			L					23
2	183.1492	92.0782			**211.1441**	106.0757			P	2616.2464	**1308.6268**	2599.2199	1300.1136	22
3	284.1969	142.6021			**312.1918**	156.5995			T	**2519.1936**	1260.1005	2502.1671	1251.5872	21
4	381.2496	191.1285			409.2445	205.1259			P	**2418.1460**	1209.5766	2401.1194	1201.0633	20
5	510.2922	255.6498			**538.2871**	269.6472			E	**2321.0932**	1161.0502	2304.0667	1152.5370	19
6	**639.3348**	320.1710			**667.3297**	334.1685			E	**2192.0506**	1096.5289	2175.0241	1088.0157	18
7	**802.3981**	401.7027			**830.3931**	415.7002			Y	**2063.0080**	1032.0076	2045.9815	1023.4944	17
8	930.4567	465.7320	913.4302	457.2187	**958.4516**	479.7295	941.4251	471.2162	Q	**1899.9447**	950.4760	**1882.9181**	941.9627	16
9	1031.5044	516.2558	1014.4779	507.7426	**1059.4993**	530.2533	1042.4728	521.7400	T	**1771.8861**	886.4467	1754.8596	877.9334	15
10	**1194.5677**	597.7875	1177.5412	589.2742	**1222.5626**	611.7850	1205.5361	603.2717	Y	**1670.8384**	835.9229	1653.8119	827.4096	14
11	1293.6361	647.3217	**1276.6096**	638.8084	**1321.6311**	661.3192	1304.6045	652.8059	V	**1507.7751**	754.3912	1490.7486	745.8779	13
12	1364.6733	682.8403	1347.6467	674.3270	**1392.6682**	696.8377	1375.6416	688.3245	A	**1408.7067**	704.8570	**1391.6801**	696.3437	12
13	1492.7318	746.8696	1475.7053	738.3563	**1520.7268**	760.8670	1503.7002	752.3537	Q	**1337.6696**	669.3384	**1320.6430**	660.8251	11
14	1591.8003	796.4038	1574.7737	787.8905	1619.7952	810.4012	1602.7686	801.8879	V	**1209.6110**	605.3091	1192.5844	596.7959	10
15	1706.8272	853.9172	1689.8006	845.4040	1734.8221	867.9147	1717.7956	859.4014	D	**1110.5426**	555.7749	**1093.5160**	547.2617	9
16	1876.9327	938.9700	1859.9062	930.4567	1904.9276	952.9675	1887.9011	944.4542	K	**995.5156**	498.2615	978.4891	489.7482	8
17	1977.9804	989.4938	1960.9539	980.9806	2005.9753	1003.4913	1988.9488	994.9780	T	**825.4101**	413.2087	808.3836	404.6954	7
18	2049.0175	1025.0124	2031.9910	1016.4991	2077.0124	1039.0099	2059.9859	1030.4966	A	**724.3624**	362.6849	707.3359	354.1716	6
19	2148.0859	1074.5466	2131.0594	1066.0333	2176.0808	1088.5441	2159.0543	1080.0308	V	**653.3253**	327.1663	636.2988	318.6530	5
20	2263.1129	1132.0601	2246.0863	1123.5468	2291.1078	1146.0575	2274.0812	1137.5443	D	**554.2569**	277.6321	537.2304	269.1188	4
21	2364.1606	1182.5839	2347.1340	1174.0706	2392.1555	1196.5814	2375.1289	1188.0681	T	**439.2300**	220.1186	422.2034	211.6053	3
22	2527.2239	1264.1156	2510.1973	1255.6023	2555.2188	1278.1130	2538.1922	1269.5998	Y	**338.1823**	169.5948	321.1557	161.0815	2
23									R	175.1190	88.0631	158.0924	79.5498	1

Figure S15. LC-MS/MS analysis of AcnB 835-AcK. The tandem mass spectrum of the peptide (residues 820-842) LPTPEEYQTYVAQVDKTAVDTYR from purified AcnB 835-AcK. KAC denotes AcK incorporation. The partial sequence of the peptide containing the AcK can be read from the annotated a/b or y ion series. Matched peaks are in red.

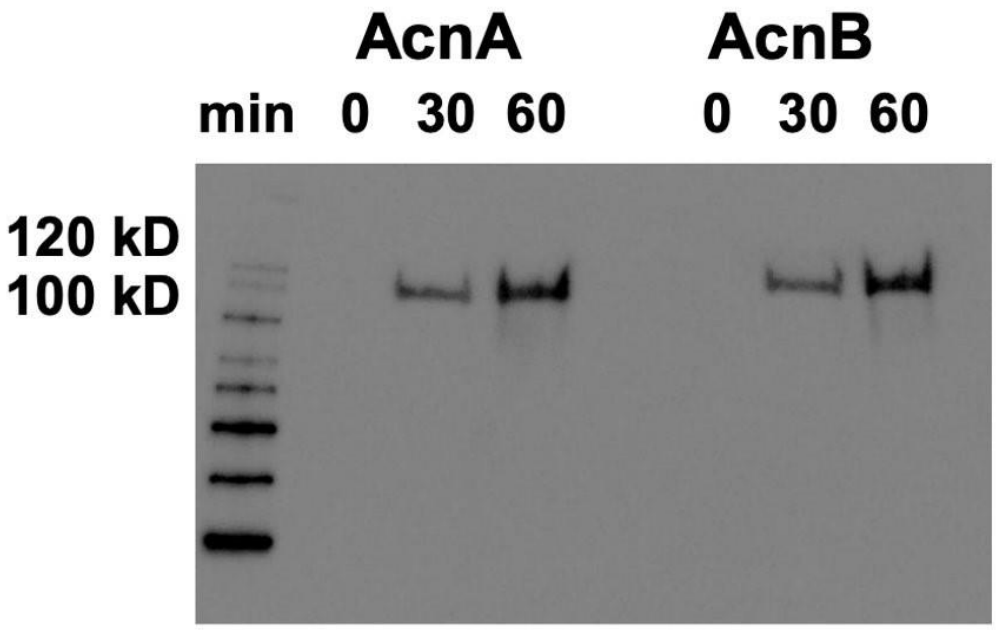

Figure S16. The full image of western blots for AcP-acetylation experiments in Figure 2A.